Thioglycosides are efficient metabolic decoys of glycosylation that reduce selectin dependent leukocyte adhesion

Shuen-Shiuan Wang [1], Xuefeng Gao [2], Virginia del Solar [1,3], Xinheng Yu [1], Aristotelis Antonopoulos [4], Alan E. Friedman [5], Eryn K. Matich [5], G. Ekin Atilla-Gokcumen [5], Mehrab Nasirikenari [6], Joseph T. Lau [6], Anne Dell [4], Stuart M. Haslam [4], Roger A. Laine [2], Khushi L. Matta [2,*] and Sriram Neelamegham [1,3,7*]

[1] Department of Chemical and Biological Engineering, [3] Clinical & Translational Research Center and [5] Chemistry, State University of New York, Buffalo, NY 14260, USA

[2] Tumor End LLC, Baton Rouge, LA 70803, USA

[4] Department of Life Sciences, Imperial College London, London SW7 2AZ, UK

[6] Department of Cellular and Molecular Biology, Roswell Park Cancer Institute, Buffalo, NY 14263, USA

[7] Lead Contact

* **Corresponding authors**: Khushi L. Matta, 340 East Parker Drive, Suite 246, Louisiana Emerging Technology Center, Baton Rouge, LA 70803, USA, Ph: +1-716-982-7262, email: klmatta40@gmail.com; Sriram Neelamegham, 906 Furnas Hall, Buffalo, NY 14260, USA; Ph: +1-716-645-1200; Fax: +1-716-645-3822; email: neel@buffalo.edu.

SUMMARY

Metabolic decoys are synthetic analogs of naturally occurring biosynthetic acceptors. These compounds divert cellular biosynthetic pathways by acting as artificial substrates that usurp the activity of natural enzymes. While O-linked glycosides are common, they are only partially effective even at millimolar concentrations. In contrast, we report that *N*-acetylglucosamine (GlcNAc) incorporated into various thioglycosides robustly truncate cell-surface N- and O-linked glycan biosynthesis at 10-100μM concentrations. The >10 fold greater inhibition is in part due to the resistance of thioglycosides to hydrolysis by intracellular hexosaminidases. The thioglycosides reduce β-galactose incorporation into lactosamine chains, cell-surface sialyl Lewis-X expression, and leukocyte rolling on selectin-substrates including inflamed endothelial cells under fluid shear. Treatment of granulocytes with thioglycosides prior to murine infusion inhibited neutrophil homing to sites of acute inflammation and bone marrow by ~80-90%. Overall, thioglycosides represent an easy to synthesize class of efficient metabolic inhibitors/decoys. They reduce N-/O-linked glycan biosynthesis and inflammatory leukocyte accumulation.

Keywords: glycosylation, glycosides, small molecule inhibitors, inflammation, selectins, fluid shear, decoy, homing, cell adhesion

INTRODUCTION

Glycans are a complex post-translational modification that regulate virtually all biological processes (Laine, 1994; Neelamegham and Mahal, 2016; Varki, 2017). Commonly, cell surface carbohydrates appear either as O- or N-linked glycans on glycoproteins, glycosphingolipids (GSLs), or glycosaminoglycans (GAGs). Such structures are formed by the sequential action of glycosyltransferases (GTs) that transfer mono- or oligo-saccharides from various donors to growing carbohydrate chains, and by glycosidases that hydrolyze individual monosaccharides to trim glycans. Small molecules developed to modify GT/glycosidase activity can lead to novel strategies to regulate glycan structures, cell function and treat diseases.

While a number of small molecule inhibitors of glycosidase activity have been developed, fewer molecules disrupt GT activity (Gloster and Vocadlo, 2012; Hudak and Bertozzi, 2014). In this regard, most small molecule GT inhibitors developed fall into one of three categories: i. Acceptor analogs of nucleotide-sugar donors or transition state mimetics of the acceptor-donor pair. While such reagents haven been shown to be effective in *in vitro* enzymology assays, their inability to permeate cell membranes limits their biological utility (Schworer and Schmidt, 2002; Zhu et al., 1995) . ii. Modified monosaccharides that are cell permeable. This large set of compounds, include monosaccharide analogs where selected hydroxyl or other groups are replaced by halogen, deoxy, thiol or methyl substituents (Goon and Bertozzi, 2002). Such molecules are often converted into their corresponding nucleotide-sugar analogs within cells, at high concentrations (Gloster et al., 2011). This results in depletion of selected, natural nucleotide-sugars, and global depression in the activities of entire families of related GTs (Rillahan et al., 2012; van Wijk et al., 2015). Thus, this approach may lack specificity. iii. Surrogate acceptors that act as artificial substrates for specific biochemical pathways (Brown et al., 2007; Sarkar et al., 1997). These molecules compete with and reduce carbohydrate biosynthesis on the natural glycoconjugate by acting as alternate substrates for the GTs. Such decoys may be designed to target specific pathways. However, to effectively compete with natural substrates, they are typically applied at relatively high concentrations. For example, peracetylated benzyl-α-GalNAc (or 'GalNAc-OBn') is added at 2-4 mM into cell culture media to inhibit O-linked glycosylation (Alfalah et al., 1999; Huet et al., 1998; Kuan et al., 1989; Tsuiji et al., 2003), and xylosides are similarly used at 1-2 mM for inhibiting GAG biosynthesis (Fritz et al., 1994; Okayama et al., 1973; Victor

et al., 2009). At lower concentrations (~10-100 μM), these decoys have little or no inhibitory activity, and thus are used as molecular probes that report on the cellular O-glycan (Kudelka et al., 2016; Stolfa et al., 2016) or GAG biosynthesis pathways (Victor et al., 2009).

In the current study, using a panel of *N*-acetylglucosamine (GlcNAc) based metabolic decoys, we observed that the efficacy of surrogate acceptors/decoys can be tuned by modifying the linkage between the carbohydrate and aglycone. In particular, the study examined the effect of modifying the acetal group found in traditional O-glycosides, to thioacetals in S-glycosides (**Figure 1A**). In this regard, previous enzymology investigations suggest that selected S- aryl glycosides are susceptible to cleavage by hexosaminidases, albeit at lower rates compared to O-glycosides (Macauley et al., 2005). In contrast, we report, here, a set of S-glycosides that are more stable with minimal breakdown by cytoplasmic, lysosomal and nuclear hexosaminidases (**Fig. 1B, 1C**). Due to this property, the S-glycosides function in cell based assays to disrupt cellular lactosamine biosynthesis on N- and O-linked glycans at ~10 fold lower concentrations compared to O-glycosides. In particular, many of the studies were performed with peracetylated compounds where the 2-naphthalenemethanol (NAP) group was linked to GlcNAc via an S-glycosidic linkage to yield 'SNAP' (compound **1**) or O-linkage to yield 'ONAP' (**7**). When added to human leukocytes, SNAP more effectively reduced expression of the sialyl Lewis-X (sLe^X, Siaα2-3Galβ1-4(Fucα1-3)GlcNAc) epitope on cells, compared to ONAP. SNAP also reduced cell adhesion to E-selectin, the major human selectin which binds sialofucosylated epitopes on leukocyte O-glycans, N-glycans and GSLs (Mondal et al., 2016; Stolfa et al., 2016). In mouse, SNAP treated leukocytes exhibited reduced migration to sites of inflammation and bone marrow. Overall, this report demonstrates the use of thioglycosides as a class of novel, potent inhibitors that can disrupt lactosamine biosynthesis on cellular O- and N-glycans.

RESULTS

Thioglycosides reduce cell surface sialyl Lewis-X expression and E-selectin binding: A panel of GlcNAc based thio/S- (**1**-**6**) and O-glycosides (**7**-**12**) were synthesized (**Figure 1A**, **Supplemental data**). The aglycone in these entities was varied. While some of the compounds contained NAP (SNAP **1**, **2**, ONAP **7**, **8**), benzyl (**6**, **12**) or bromooctane (**5**) aglycones, others contained derivatives of natural products, geranyl (**3**, **4**, **11**) or methoxyphenyl (**9**, **10**). Several of the compounds were peracetylated (**1**, **3**, **5**, **6**, **7**, **9**) to enhance cell permeability (Sarkar et al., 1997). The acetyl groups are removed by esterases inside cells to yield free carbohydrates (**Fig. 1B, 1C**).

We determined if any of the compounds alter cell surface glycans important for inflammatory cell adhesion (**Figure 2**). Here, treatment of HL-60 promyelocytic leukemia cells with 100 μM of all S-glycosides for 40h reduced cell surface sialyl Lewis-X (sLe^X) expression by 60-90% as measured using mAb HECA-452 (**Fig. 2A**). The results with O-glycosides was more variable with (**11**) and (**7**) reducing the sLe^X epitope by 20% and 40%, and (**10**) augmenting sLe^X by 30%. Upon comparing the GlcNAc-β-SNAP in its peracetylated (SNAP, **1**) vs. free (**2**) form, it is apparent that peracetylation is not critical for inhibition function although it improves efficacy. Thus the NAP group exhibits sufficient hydrophobicity for cell permeability, and additional acetylation of glycan hydroxyl groups only has a marginal contribution. S-glycosides were effective at concentrations as low as 10 μM with maximum effectiveness above 50 μM (**Fig. 2B**).

As sLe^X is a critical determinant for selectin-dependent leukocyte adhesion, the effect of the S- and O-glycosides on soluble human selectin-IgG protein binding to HL-60s was assayed. Here, consistent with the HECA-452 measurements, all S-glycosides reduced E-selectin-IgG binding, with the blocking pattern being remarkably similar to the changes in sLe^X expression (**Fig. 2C, 2D**). The O-glycosides did not exhibit this property. Similar to E-selectin, many of the S-glycosides (**1-3**, **5**, **6**) also down-regulated L-selectin binding though the effect was smaller (**Fig. 2E**). None of the glycosides affected P-selectin binding (**Fig. 2F**). The core-2 sLe^X epitope at the *N*-terminus of PSGL-1 is the major P-selectin ligand on human leukocytes (Lo et al., 2013; Wilkins et al., 1996), and this structure is apparently not fully disrupted by the compounds. Function blocking anti-selectin mAbs and vehicle controls confirm the specificity of the

measured interaction. Cytometry histograms suggests that these observations are true for the entire cell population, and not limited to a sub-population of HL-60s (**Supplemental Fig. S1**).

Similar to the undifferentiated HL-60s, SNAP also reduced sLe^X expression and E-selectin binding to neutrophils obtained by terminal-differentiation of HL-60s using DMSO (**Supplemental Fig. S2**). These differentiated cells expressed five-times greater cell surface CD11b levels compared to undifferentiated HL-60s, with CD11b expression being unaffected by the glycoside treatment (**Fig. S2A**). Thus, the glycosides do not alter the overall cell phenotype. Here, also, SNAP (S-glycoside) reduced sLe^X expression by 70% (**Fig. S2B**), E-selectin binding by 85% (**Fig. S2C**) and L-selectin IgG recognition by 30% (**Fig. S2D**), without altering P-selectin (**Fig. S2E**). Neither SNAP nor ONAP altered leukocyte surface expression of putative selectin-ligand scaffolds: CD11b, CD43, CD44, CD45 or CD162 (data not shown). Overall, the S-glycosides are potent modifiers of glycan biosynthesis.

Thio/S-glycosides reduce leukocyte adhesion under hydrodynamic shear: Among the compounds tested, many of the studies contrasted the effectiveness of SNAP (**1**) with respect to ONAP (**7**) since both molecules are peracetylated, and they are prototypic members of the S- and O-glycoside families. Neither compound, up to 200 μM, affected cell viability or proliferation based on trypan-blue exclusion, LDS-751 live cell staining, hemocytometer counts, or the tetrazolium salt based XTT assay (data not shown). Also, none of the treatments promoted apoptosis based on Annexin-V binding (data not shown).

Microfluidics-based leukocyte adhesion measurements determined if the reduced selectin-binding observed in the static assays, translate to physiologically relevant fluid shear conditions (**Figure 3**). Here, glycoside or control treatments did not alter the density of rolling or adherent cells on substrates composed of E-selectin bearing IL-1β simulated HUVECs (**Fig. 3A**), immobilized E-selectin (**Fig. 3B**), L-selectin (**Fig. 3C**) or P-selectin (**Fig. 3D**). However, SNAP increased the median cell rolling velocity on E-selectin bearing stimulated HUVEC monolayers by 4.5-fold (from 1 μm/s to 4.5 μm/s, **Fig. 3E**), on E-selectin substrates by 2-fold (from 2.4 μm/s to 4.33 μm/s, **Fig. 3F**) and on L-selectin by 3-fold (from 18 μm/s to 53 μm/s, **Fig. 3G**). The glycoside did not affect rolling on P-selectin (**Fig. 3H**). These observations were confirmed at multiple

glycoside concentrations, 25-100μM (**Fig. S2F-G**). Overall, SNAP reduced leukocyte interactions on E-selectin and stimulated endothelial cells.

SNAP abrogated neutrophil homing to sites of inflammation and the bone marrow in mice: Previous studies show that increased rolling velocity on selectins *ex vivo* may be sufficient to reduce leukocyte accumulation *in vivo* (Marathe et al., 2010; Morikis et al., 2017). To determine the anti-inflammatory potential of the S-glycosides, a murine thioglycollate peritonitis model was used to contrast the effect of SNAP *vs*. ONAP (**Figure 4**). Here, murine bone marrow cells (mBMCs) obtained from donor C57BL/6 were cultured *ex vivo* with either ONAP, SNAP or vehicle for 40 h (**Fig. 4A**). These cells were then differentially labeled with either a green fluorescent dye (CMFDA), red dye (CMTMR) or both to result in three differentially stained cell populations. The populations were mixed in equal proportion. Peritonitis was induced in recipient C57BL/6 using thioglycollate *i.p.* injection for 1 h, and then the labeled cell mixture was introduced *i.v.*. At 20h, 20-30% fewer ONAP treated cells were observed in the bone marrow and inflamed peritoneum, compared to vehicle treatment (**Fig. 4B-4D**). SNAP caused a more dramatic decrease, with cell accumulation being consistently reduced by ~80-90%. Deficiency in E- and L-selectin dependent cell adhesion may contribute to the observed reduced homing to sites of inflammation.

Upregulation of PNA and ECL lectin binding upon treatment with S-glycosides: Flow cytometry based lectin binding studies were performed, to identify reagents that quantitatively report on the effect of glycoside treatment in heterologous cell types (**Figure 5**). Here, SNAP augmented PNA binding to HL-60s by ~30 fold suggesting the alteration of O-linked glycan biosynthesis, and the increased expression of the Galβ1,3GalNAc epitope (**Fig. 5A**). A ~5-fold increase in ECL binding (**Fig. 5B**) and doubling of PHA-L binding (**Fig. 5C**) was also measured indicating potential perturbations in N-glycan structures, particularly the Galβ1,4GlcNAc lactosamine chains. Additionally, anti-Le^X mAb binding was marginally decreased (**Fig. 5D**). More prominent changes in lectin binding accompanied SNAP treatment, compared to ONAP (**Fig. 5**). In such studies, PNA, ECL and PHA-L lectin binding to O- and N-glycans is typically augmented upon de-

sialylation (Stolfa et al., 2016). However, the MAL-II binding data indicate that the overall expression of α2,3 sialic acid terminated glycans remains unchanged.

In general, the entire panel of S-glycosides exhibited a pattern of carbohydrate epitope alteration similar to SNAP, albeit to varying degrees depending on the aglycone (**Supplemental Fig. S3**). All O-glycosides were similar to vehicle control except for ONAP (**7**) which displayed some carbohydrate modification potential, although low relative to SNAP. The increased PNA-lectin binding upon SNAP treatment was observed across multiple cell lines, including human embryonic kidney HEK293T, breast cancer T47D and ZR75-1, and prostate PC-3 cells (**Supplemental Fig. S4A**). Similar to undifferentiated HL-60s, HL-60s differentiated to neutrophils also exhibited >10-fold increase in PNA-binding following culture with SNAP (**Supplemental Fig. S4B**). Significantly, the concentration range where selectin-binding function was altered in Fig. 2-4 was similar to that necessary for PNA-lectin binding alteration (20-100 μM, **Supplemental Fig. S4C**). Thus, all S-glycosides appear to alter cellular glycosylation via similar molecular mechanisms.

Truncation of O-glycan biosynthesis by S-glycosides: The increased PNA-lectin binding suggests that the S-glycosides may modify cell surface O-glycans. This was confirmed using a panel of CRISPR-Cas9 knockout cell lines since PNA-lectin binding to leukocytes was abolished in cells lacking O-glycans under a variety of conditions, including upon SNAP treatment (**Supplemental Fig. S5A-B**). In addition, the S-glycoside reduced the molecular mass of two prominent leukocyte glycoproteins, PSGL-1 which is the major L-/P-selectin ligand (**Fig. 5E**) and CD43/leukosialin (**Fig. 5F**). Both mucin glycoproteins displayed a ~20% reduction in molecular mass upon SNAP, but not ONAP, treatment.

To determine the biosynthetic steps affected by SNAP, radioactivity based ppGalNAc-transferase (**Supplemental Fig. S5C**) and β1,3GalT (**Fig. 5G**) enzymology assays were undertaken. Here, lysates of cells cultured with decoys or controls served as the enzyme source. Cell lysates were mixed with radioactive donor (UDP-[^{14}C]GalNAc or UDP-[^{14}C]Gal) along with synthetic substrates, *N*-terminal PSGL-1 peptide for ppGalNAcT and GalNAc-O-Bn for GalT. Enzymatic transfer of radioactivity from donor to substrate was

then measured. Here, the transfer of [^{14}C]GalNAc to the peptide substrate was similar in all lysates suggesting that the glycosides may not alter ppGalNAcT activity.

In the GalT assay, however, two distinct products were observed using thin layer chromatography (TLC) when the lysates contained ONAP or SNAP (left half, **Fig. 5G**). One migrated identically to [^{14}C]Galβ1,3GalNAc-O-Bn, while the second migrated faster. This second product is likely [^{14}C]Gal-GlcNAc-S-NAP (lane 2) and [^{14}C]Gal-GlcNAc-O-NAP (lane 3) formed using unprocessed SNAP and ONAP available in cell lysates, as these same entities were also prominently observed upon omitting GalNAc-O-Bn in the reaction mixture (right half, **Fig. 5G**). The extent of [^{14}C]Gal transfer to SNAP was ~2-fold greater than that to ONAP based on the more intense radioactive product. Even when GalNAc-O-Bn was present in the reaction mixture (left half, **Fig. 5G**), [^{14}C]Gal-GlcNAc-S-NAP was the dominant product in the SNAP runs, while equal amounts of [^{14}C]Gal-GlcNAc-O-NAP and [^{14}C]Galβ1,3GalNAc-O-Bn were formed in the ONAP run. Independent MS-based enzymology studies suggest that these observations are not simply because SNAP is a superior acceptor for galactose compared to ONAP (**Fig. S5D**). In these runs, Gal transfer to ONAP was also diminished in the presence of SNAP, suggesting a potential inhibitory function for the S-glycoside (Brockhausen et al., 2006). Overall, the S-glycosides may act both as acceptors of galactose and inhibitors of related enzymes.

Mass spectrometry studies were undertaken to determine the effect of SNAP and ONAP on O-glycosylation using the cellular O-glycan reporter assay (Kudelka et al., 2016). Here, peracetylated GalNAc-O-Bn was fed to cells in the presence of glycosides or control, and products formed on these substrates was quantified using MS by assaying the culture medium (**Fig. 5H-J**, all structures validated using MS/MS). Here, 38% of the GalNAc-O-Bn substrate was converted to other products when media contained GalNAc/control (**Fig. 5H**). Products formed included Galβ1-3GalNAc-OBn/T-antigen, mono- and di-sialylated T-antigen, and core-2 glycans. The fraction of GalNAc-O-Bn converted to product was reduced to 14% upon culture with ONAP and 2.5% upon SNAP addition. Thus, T-antigen biosynthesis was inhibited by the S-glycoside decoy. Consistent with this notion, VVA-lectin binding (recognizes GalNAcα on O-glycans) to HL-60s treated with the entire panel of S-glycosides was augmented by 3-100 fold (**Supplemental Fig S6**). The effect of the O-glycosides was small, in comparison. In addition to GalNAc-O-Bn, a variety of glycan products were also elaborated on SNAP (**Fig. 5I**) and ONAP (**Fig. 5J**), including

sLe^X structures, and extended LacNAc chains sometimes containing terminal fucose and sialic acid. Whereas elaborated glycans were observed on 23% of the SNAP substrate in the culture medium, this was lower at 17% for ONAP.

SNAP truncates N- and O-glycan biosynthesis, with a smaller effect on glycolipids: MALDI-TOF MS glycome profiling was undertaken to determine the precise N- and O-glycans, and GSLs that are altered by SNAP (**Figure 6**). Here, we observed an increased abundance of GlcNAc terminated (agalactosylated, truncated) carbohydrate chains and LacNAc antennas with reduced sialic acid abundance (red peaks in **Fig. 6A**, lower panel). These characteristic desialylated peaks that appear at *m/z* 2530, 2734 etc. may explain the increased ECL binding in Fig. 5B. N-glycans from SNAP treated HL60s also displayed the absence of the sLe^X epitope (**Fig. 6B**), consistent with the reduced expression of the HECA-452 epitope (**Fig. 2A**). Notably, bi- and tri-antennary glycans with the sLe^X epitope (*m/z*=3140, 3950) are apparent in the vehicle, but not SNAP treated cells.

The effect of SNAP on the GSLs was small, compared to that on the N-glycans. Here, a majority of the GSL glycans were similar in vehicle *vs*. SNAP. However, a few truncated glycans were also apparent at *m/z*=1188, 1566 and 2087 (red peaks in **Fig. 6C**, lower panel). Sialylated GSL glycans were also reduced upon SNAP treatment compared to vehicle control, *e.g*. the peak ratio at *m*/*z* 1304/943 was reduced from 1.64 in vehicle to 0.56 upon SNAP treatment; and at *m*/*z* 1753/1392 from 1.28 in vehicle to 0.92 for SNAP (**Fig. 6C**, upper and lower panels). Finally, consistent with the observations using GalNAc-O-Bn, O-glycans from SNAP treated HL60s revealed a loss of core-1 and core-2 structures (**Fig. 6D**).

SNAP is a more potent surrogate acceptor-decoy compared to ONAP: The more potent inhibitory effect of SNAP compared to ONAP, could be due to the inherent intracellular stability of S-glycosides. In this regard, O-glycosides are commonly used to assay the activity of hexosaminidases, and it is known that mammalian cells have lysosomal, nuclear and cytoplasmic hexosaminidases that may cleave such substrates (Stutz and Wrodnigg, 2016). To determine if such hexosaminidase activity is prominent in HL-60 cells, we measured the HPLC elution profile of 2-napthelenemethanol (HONAP, hydrolyzed ONAP) and

2-naphthalenemethanethiol (HSNAP) standards spiked into the HL-60 cell culture supernatant (**Fig. 7A**). This profile was compared to that of cells cultured with vehicle (**Fig. 7B**), ONAP (**Fig. 7C**) and SNAP (**Fig. 7D**). Here, a prominent peak with retention time corresponding to HONAP was observed in Fig. 7C upon culture with ONAP, but not one corresponding to HSNAP in Fig. 7D when SNAP was present. Based on area-under-the-curve, recoveries, and absorbance calibration curves generated with chemical standards, we estimate that ~30% of ONAP may be cleaved within cells. Neither LC-MS nor GC-MS were able to ionize underivatized HONAP for MS detection, and thus dansylated-HONAP standards were prepared (**Fig. 7E-F**). Additionally, NAP products secreted into cell culture medium were also derivatized with dansyl chloride (**Fig. 7G**). Here, ESI-Q-ToF MS/MS was able to verify the formation of HONAP by HL-60s, based on retention time compared to chemical standards (**Fig. 7F** *vs*. **7G**, left panels), mass and also fragmentation spectra (right panels). Overall, ONAP and/or its derivatives are partially hydrolyzed in cells, while SNAP is not.

To determine the nature of competition between the glycosides, equal amounts of peracetylated ONAP and SNAP were mixed and fed to HL-60 cell culture medium. At 40h, glycoside products were purified from culture supernatants (**Fig. 7H**) and cell pellets (**Fig. 7I**). They were permethylated and quantified based on product ion counts using high-resolution LC-MS/MS. As seen, the total prevalence of extra- and intra-cellular glycoside-products was greater in the presence of SNAP compared to ONAP, suggesting a role for hydrolysis in regulating relative glycan biosynthesis. In particular, the concentration of SNAP substrate was 2.8 fold higher in the pellet compared to ONAP. In addition, whereas a variety of products were synthesized when ONAP was fed to cells alone (Fig. 5J), glycan elaboration on this substrate was diminished in mixed systems that contained SNAP (Fig. 7H-I). 8-14 fold higher levels of glycans were formed on SNAP compared to ONAP. Similar observations were made in independent validation runs performed using ESI-Q-ToF MS (**Supplemental Fig. S7**). Overall, the hydrolysis of O-glycosides may partially explain the reduced efficacy of such compounds, compared to the S-glycosides.

DISCUSSION

This study demonstrates that thioglycosides or S-glycosides efficiently disrupt cellular biosynthetic pathways important for inflammatory processes by functioning as metabolic decoys. This was observed in multiple cell types including leukocytes (HL-60s and primary leukocytes), breast (T47D, ZR75-1) and prostate (PC3) cells. Such decoys were effective at low concentrations of ~10-100 µM. In contrast, the more common O-glycosides are only functional at >10 fold higher doses. The enhanced functional efficacy of S-glycosides was noted in all assays, and it was most apparent in the competition/co-culture assay where SNAP and ONAP were simultaneously fed to cells. Here, MS-analysis of biosynthetic products present in culture medium and cell pellet showed that extended glycosylation products formed on SNAP with 8-14 fold greater efficacy compared to ONAP. Indeed, while there is literature on the synthesis of S-glycosides, and alkyl/aryl 1-thioglycosides are used as donors during the chemical synthesis of carbohydrates, relatively fewer studies have applied such compounds in cell based assays (Macauley et al., 2005; Miura et al., 1999). The current results suggest that this may be a valuable avenue for investigation, as it can yield entities that can modify cellular biosynthetic pathways and related glycan structures. The scale up of such compounds is cost-effective.

All S-glycosides used in this study truncate lactosamine chain extensions on N-glycans and O-glycans, though their relative efficacy varied depending on the aglycone. In this regard, SNAP affected both Type-III Galβ1,3GalNAc chains on O-glycans based on the increased binding of VVA and PNA, and Type-II Galβ1,4GlcNAc chains on N-glycans based on alterations in ECL binding (Stolfa et al., 2016). MS-based glycomics profiling also showed an increase in GlcNAc terminated N-glycans and reduction in sialyllactosamine structures on N-glycans. These glycomics profiles are reminiscent of previous cases of Congenital Disorders of Glycosylation (Boztug et al., 2014; Hayee et al., 2011). The sLe^X structure was prominently absent in the SNAP samples. Lactosamine extensions on O-glycans were also reduced upon S-glycoside treatment as the carbohydrates synthesized on the GalNAc-O-Bn substrate were small. Immunoblotting showed that the molecular mass of two mucinous proteins, PSGL-1 and CD43, was reduced upon S-glycoside addition. Thus, the overall glycan mass on extended O-glycans and N-glycans was reduced. The effect of the compound on GSLs was relatively small.

Regarding the mechanism of action, the data suggest that the thioglycosides may be superior decoys due to their enhanced stability in cells, and reduced susceptibility to degradation by mammalian β-hexosaminidases (EC 3.2.1.52). Additionally, these glycosides may inhibit specific GalT activity (Brockhausen et al., 2006), though the mechanism for this process and specificity toward different members of this enzyme class remains unsolved (Gao et al., 2010). Consistent with the dual role for S-glycosides as decoys and inhibitors, while equal amounts of [C^{14}]Gal were transferred to ONAP and GalNAc-O-Bn in the GalT assay, SNAP acted as an efficient decoy to take up almost ~90% of the [C^{14}]Gal and it dramatically reduced [C^{14}]Galβ1,3GalNAc-OBn formation. In this regard, hexosaminidases in cells are present in the lysosomal, cytoplasmic and nuclear compartments in humans and may contribute to the degradation of O-glycosides and their products, including those containing terminal GlcNAc and GalNAc (Mahuran, 1999). Here, the lysosome contains various isoenzymes (HexA, HexB and HexS) that are synthesized by the homo- or hetero- dimerization of two subunits: α encoded by HEXA and β by HEXB. Mutations in HEXB often results in Sandhoff disease, while mutations in HEXA decreases GM2 ganglioside degradation and causes Tay-Sachs disease (Sandhoff and Harzer, 2013). HEXC encodes for O-GlcNAcase (OGA) which acts as a nucleocytoplasmic β-hexosaminidase that removes O-GlcNAc modification on various proteins (Gao et al., 2001). Mammalian cells also contain a fourth hexosaminidase HexD in the nucleus and cytoplasm, encoded by HEXDC (Gutternigg et al., 2009), which prefers to hydrolyze GalNAc compared to GlcNAc (Alteen et al., 2016). Additional studies are needed to determine which of the hexosaminidases act on ONAP and other O-glycosidase substrates as this may be a key mitigating factor that reduces the efficacy of such compounds.

The mammalian lactosamine motif is a common unit that is part of the molecular recognition epitope of various lectins, including selectins, siglecs and galectins (Neelamegham and Mahal, 2016; Varki, 2017). As GlcNAc based S-glycosides truncate the growth of this common motif on different types of glycoconjugates, these small molecules may be broadly useful as inhibitors for a variety of studies, although this may come at the cost of reduced specificity. To demonstrate such biological utility, we tested the ability of SNAP and ONAP to reduce selectin-dependent cell adhesion with focus on E-selectin, an endothelial lectin that binds sialofucosylated glycans like sLe^X on all common glycoconjugate-types: O-glycans, N-glycans and GSLs (Stolfa et al., 2016). Here, all S-glycosides dramatically reduced cell surface leukocyte

sialyl Lewis-X expression on leukocytes, and E- and L-selectin binding under static and flow conditions. These compounds also increased leukocyte rolling velocity on stimulated endothelial cell monolayers, and treatment of leukocytes with these compounds abolished transplanted cell homing to the bone marrow and sites of inflammation in mouse. This effect of small molecules to reduce inflammation by altering leukocyte rolling rates is similar to results noted using two different sialyl Lewis-X analogs that completed Phase II trials, GMI-1070 (Rivipansel) (Morikis et al., 2017) and TBC-1269 (Hicks et al., 2005), and also the monosaccharide-analog 4F-GalNAc (Marathe et al., 2010). In the case of Rivipansel, a molecule currently in Phase III trials for reducing vaso-occlusive crisis following sickle cell disease, the partial reduction of E-selectin binding interactions is considered to reduce cell activation via selectin-ligand interactions (Morikis et al., 2017). This alteration in cell activation rather than the complete abrogation of selectin-ligand interaction is considered to be the mechanism of molecular action. Consistent with this notion, SNAP also dramatically reduced cell migration to sites of inflammation and the bone marrow in the current study, by modifying leukocyte rolling interactions in flow assays. Additional studies are needed *in vivo* to complete the pharmacological characterization of the S-glycosides, compare their blocking efficacy to other small molecule selectin antagonists (Dimitroff et al., 2003; Marathe et al., 2010; Rillahan et al., 2012; Sarkar et al., 1997; Zandberg et al., 2012), and to test their inhibitory efficacy in relevant diseases models.

In conclusion, this study suggests that thioglycosides may be suitable for a broad range of basic science and translational investigations, due to their enhanced efficacy within cells compared to the O-glycosides. Using SNAP as a prototypic entity, it may be possible to vary the aglycone group to create molecular entities with varying specificity for diverse applications. Advancing this concept, the glycan/GlcNAc entity of SNAP may also be changed to target other glycan biosynthetic pathways. Finally, it may be valuable to also vary the anomeric linkage in order to further enhance functional effects. Such modifications to the glycan, linkage and aglycone may result in novel tools for biomedical research and drug candidates with favorable pharmacological activity to target leukocyte adhesion, inflammation and cancer metastasis.

SIGNIFICANCE

There is active interest in rationally designing small molecule inhibitors of cellular glycosylation. One such approach uses metabolic decoys that function as mimetics of naturally occurring glycoEnzyme (glycosylating enzyme) substrates. When introduced into cells, such decoys attract the activity of the glycoEnzymes and thus the natural glycoconjugates are left under-glycosylated. This manuscript demonstrates that the simple chemical modification of the anomeric linkage of metabolic decoys, from acetal in traditional O-glycosides to thioacetal group in thio/S-glycosides, dramatically enhances the stability of these compounds within cells and improves inhibitor efficacy by >10 fold. This strategy to improve metabolic decoy design may enhance their application in basic science studies, and also clinical investigations as anti-inflammatory, anti-metastasis and anti-viral therapies.

Acknowledgements: Supported by the NIH SBIR grant GM106513 to KLM, NIH awards HL103411 and GM126537 to SN, NHLBI Program of Excellence in Glycosciences grant HL107146 to JTYL, and the Biotechnology and Biological Sciences Research Council Grant BB/K016164/1 to AD and SMH. Orbitrap MS studies were supported by the BioDesign Core, University at Buffalo.

Author contributions: Conceptualization, K.L.M., S.N.; Writing-Original Draft: S.S.W., S.N.; Writing-Review and Editing: all authors; Supervision: G-E.A.G., J.T.L., A.D., S.M.H., K.L.M., S.N.; Investigation and Methodology: S.S.W., X.G., V.dS, X.Y., A.A., A. E.F., E.K.M., M.N.; Validation: V.dS, E.K.M.; Resources: X.G., R.A.L., K.L.M.; Funding Acquisition: J.T.L., A.D., S.M.H., R.A.L., K.L.M., S.N.; Co-Corresponding authors: K.L.M. lead the chemical synthesis effort. S.N. lead functional studies.

Declaration of interests: X.G., K.L.M. and R.A.L. are affiliated with TumorEnd LLC, a for-profit small business with interest in anti-inflammatory molecules. These investigators synthesized the tested compounds and requested but did not perform any testing. K.L.M. authored PCT WO/2016/077567 related to the use of glycosides for anti-inflammatory-/viral- activity. All other authors declare no conflicts of interest.

Reference

Alfalah, M., Jacob, R., Preuss, U., Zimmer, K.P., Naim, H., and Naim, H.Y. (1999). O-linked glycans mediate apical sorting of human intestinal sucrase-isomaltase through association with lipid rafts. Curr Biol *9*, 593-596.

Alteen, M.G., Oehler, V., Nemcovicova, I., Wilson, L.B.H., Vocadlo, D.J., and Gloster, T.M. (2016). Mechanism of Human Nucleocytoplasmic Hexosaminidase D. Biochemistry *55*, 2735-2747.

Boztug, K., Jarvinen, P.M., Salzer, E., Racek, T., Monch, S., Garncarz, W., Gertz, E.M., Schaffer, A.A., Antonopoulos, A., Haslam, S.M*., et al.* (2014). JAGN1 deficiency causes aberrant myeloid cell homeostasis and congenital neutropenia. Nat Genet *46*, 1021-1027.

Brockhausen, I., Benn, M., Bhat, S., Marone, S., Riley, J.G., Montoya-Peleaz, P., Vlahakis, J.Z., Paulsen, H., Schutzbach, J.S., and Szarek, W.A. (2006). UDP-Gal: GlcNAc-R beta1,4-galactosyltransferase--a target enzyme for drug design. Acceptor specificity and inhibition of the enzyme. Glycoconj J *23*, 525-541.

Brown, J.R., Crawford, B.E., and Esko, J.D. (2007). Glycan antagonists and inhibitors: a fount for drug discovery. Crit Rev Biochem Mol Biol *42*, 481-515.

Buffone, A., Jr., Mondal, N., Gupta, R., McHugh, K.P., Lau, J.T., and Neelamegham, S. (2013). Silencing alpha1,3-fucosyltransferases in human leukocytes reveals a role for FUT9 enzyme during E-selectin-mediated cell adhesion. J Biol Chem *288*, 1620-1633.

Ceroni, A., Maass, K., Geyer, H., Geyer, R., Dell, A., and Haslam, S.M. (2008). GlycoWorkbench: a tool for the computer-assisted annotation of mass spectra of glycans. J Proteome Res *7*, 1650-1659.

Cheng, K., Zhou, Y., and Neelamegham, S. (2017). DrawGlycan-SNFG: a robust tool to render glycans and glycopeptides with fragmentation information. Glycobiology *27*, 200-205.

Claeyssens, M., Kersters-Hilderson, H., Van Wauwe, J., and De Bruyne, C.K. (1970). Purification of Bacillus pumilus beta-D-xylosidase by affinity chromatography. FEBS Lett *11*, 336-338.

Dimitroff, C.J., Kupper, T.S., and Sackstein, R. (2003). Prevention of leukocyte migration to inflamed skin with a novel fluorosugar modifier of cutaneous lymphocyte-associated antigen. J Clin Invest *112*, 1008-1018.

Fettke, A., Peikow, D., Peter, M.G., and Kleinpeter, E. (2009). Synthesis and conformational analysis of glycomimetic analogs of thiochitobiose. Tetrahedron *65*, 4356-4366.

Folch, J., Lees, M., and Sloane Stanley, G.H. (1957). A simple method for the isolation and purification of total lipides from animal tissues. J Biol Chem *226*, 497-509.

Fritz, T.A., Lugemwa, F.N., Sarkar, A.K., and Esko, J.D. (1994). Biosynthesis of heparan sulfate on beta-D-xylosides depends on aglycone structure. J Biol Chem *269*, 300-307.

Gao, Y., Lazar, C., Szarek, W.A., and Brockhausen, I. (2010). Specificity of beta1,4-galactosyltransferase inhibition by 2-naphthyl 2-butanamido-2-deoxy-1-thio-beta-D-glucopyranoside. Glycoconj J *27*, 673-684.

Gao, Y., Wells, L., Comer, F.I., Parker, G.J., and Hart, G.W. (2001). Dynamic O-glycosylation of nuclear and cytosolic proteins: cloning and characterization of a neutral, cytosolic beta-N-acetylglucosaminidase from human brain. J Biol Chem *276*, 9838-9845.

Gloster, T.M., and Vocadlo, D.J. (2012). Developing inhibitors of glycan processing enzymes as tools for enabling glycobiology. Nat Chem Biol *8*, 683-694.

Gloster, T.M., Zandberg, W.F., Heinonen, J.E., Shen, D.L., Deng, L., and Vocadlo, D.J. (2011). Hijacking a biosynthetic pathway yields a glycosyltransferase inhibitor within cells. Nat Chem Biol *7*, 174-181.

Goon, S., and Bertozzi, C.R. (2002). Metabolic substrate engineering as a tool for glycobiology (Reprinted from Glycochemistry: Principles, Synthesis, and Applications, pg 641-674, 2001). J Carbohydr Chem *21*, 943-977.

Gutternigg, M., Rendic, D., Voglauer, R., Iskratsch, T., and Wilson, I.B. (2009). Mammalian cells contain a second nucleocytoplasmic hexosaminidase. Biochem J *419*, 83-90.

Hayee, B., Antonopoulos, A., Murphy, E.J., Rahman, F.Z., Sewell, G., Smith, B.N., McCartney, S., Furman, M., Hall, G., Bloom, S.L.*, et al.* (2011). G6PC3 mutations are associated with a major defect of glycosylation: a novel mechanism for neutrophil dysfunction. Glycobiology *21*, 914-924.

Hicks, A.E., Abbitt, K.B., Dodd, P., Ridger, V.C., Hellewell, P.G., and Norman, K.E. (2005). The anti-inflammatory effects of a selectin ligand mimetic, TBC-1269, are not a result of competitive inhibition of leukocyte rolling in vivo. J Leukoc Biol *77*, 59-66.

Horton, D., and Wolfrom, M.L. (1962). Thiosugars .1. Synthesis of derivatives of 2-amino-2-deoxy-1-thio-D-glucose. J Org Chem *27*, 1794-1800.

Hudak, J.E., and Bertozzi, C.R. (2014). Glycotherapy: new advances inspire a reemergence of glycans in medicine. Chem Biol *21*, 16-37.

Huet, G., Hennebicq-Reig, S., de Bolos, C., Ulloa, F., Lesuffleur, T., Barbat, A., Carriere, V., Kim, I., Real, F.X., Delannoy, P.*, et al.* (1998). GalNAc-α-O-benzyl inhibits NeuAcα2-3 glycosylation and blocks the intracellular transport of apical glycoproteins and mucus in differentiated HT-29 cells. J Cell Biol *141*, 1311-1322.

Ibatullin, F.M., Selivanov, S.I., and Shavva, A.G. (2001). A general procedure for conversion of S-glycosyl isothiourea derivatives into thioglycosides, thiooligosaccharides and glycosyl thioesters (pg 419, 2001). Synthesis-Stuttgart, 1110-1110.

Kuan, S.F., Byrd, J.C., Basbaum, C., and Kim, Y.S. (1989). Inhibition of mucin glycosylation by aryl-N-acetyl-alpha-galactosaminides in human colon cancer cells. J Biol Chem *264*, 19271-19277.

Kudelka, M.R., Antonopoulos, A., Wang, Y., Duong, D.M., Song, X., Seyfried, N.T., Dell, A., Haslam, S.M., Cummings, R.D., and Ju, T. (2016). Cellular O-Glycome Reporter/Amplification to explore O-glycans of living cells. Nat Methods *13*, 81-86.

Laine, R.A. (1994). A calculation of all possible oligosaccharide isomers both branched and linear yields 1.05 x 10(12) structures for a reducing hexasaccharide: the Isomer Barrier to development of single-method saccharide sequencing or synthesis systems. Glycobiology *4*, 759-767.

Lo, C.Y., Antonopoulos, A., Gupta, R., Qu, J., Dell, A., Haslam, S.M., and Neelamegham, S. (2013). Competition between core-2 GlcNAc-transferase and ST6GalNAc-transferase regulates the synthesis of the leukocyte selectin ligand on human P-selectin glycoprotein ligand-1. J Biol Chem *288*, 13974-13987.

Macauley, M.S., Stubbs, K.A., and Vocadlo, D.J. (2005). O-GlcNAcase catalyzes cleavage of thioglycosides without general acid catalysis. J Am Chem Soc *127*, 17202-17203.

Mahuran, D.J. (1999). Biochemical consequences of mutations causing the GM2 gangliosidoses. Biochim Biophys Acta *1455*, 105-138.

Marathe, D.D., Buffone, A., Jr., Chandrasekaran, E.V., Xue, J., Locke, R.D., Nasirikenari, M., Lau, J.T., Matta, K.L., and Neelamegham, S. (2010). Fluorinated per-acetylated GalNAc metabolically alters glycan structures on leukocyte PSGL-1 and reduces cell binding to selectins. Blood *115*, 1303-1312.

Marathe, D.D., Chandrasekaran, E.V., Lau, J.T., Matta, K.L., and Neelamegham, S. (2008). Systems-level studies of glycosyltransferase gene expression and enzyme activity that are associated with the selectin binding function of human leukocytes. FASEB J *22*, 4154-4167.

Matta, K.L., Johnson, E.A.Z., Girotra, R.N., and Barlow, J.J. (1973). Synthesis of 2-Acetamido-2-Deoxy-1-Thio-β-D-Glucopyranosides. Carbohydr Res *30*, 414-417.

Miura, Y., Kim, S., Etchison, J.R., Ding, Y., Hindsgaul, O., and Freeze, H.H. (1999). Aglycone structure influences alpha-fucosyltransferase III activity using N-acetyllactosamine glycoside acceptors. Glycoconj J *16*, 725-730.

Mondal, N., Buffone, A., Jr., Stolfa, G., Antonopoulos, A., Lau, J.T., Haslam, S.M., Dell, A., and Neelamegham, S. (2015). ST3Gal-4 is the primary sialyltransferase regulating the synthesis of E-, P-, and L-selectin ligands on human myeloid leukocytes. Blood *125*, 687-696.

Mondal, N., Stolfa, G., Antonopoulos, A., Zhu, Y., Wang, S.S., Buffone, A., Jr., Atilla-Gokcumen, G.E., Haslam, S.M., Dell, A., and Neelamegham, S. (2016). Glycosphingolipids on Human Myeloid Cells Stabilize

E-Selectin-Dependent Rolling in the Multistep Leukocyte Adhesion Cascade. Arterioscler Thromb Vasc Biol *36*, 718-727.

Morikis, V.A., Chase, S., Wun, T., Chaikof, E.L., Magnani, J.L., and Simon, S.I. (2017). Selectin catch-bonds mechanotransduce integrin activation and neutrophil arrest on inflamed endothelium under shear flow. Blood *130*, 2101-2110.

Mukherjee, D., Ray, P.K., and Chowdhury, U.S. (2001). Synthesis of glycosides via indium(III) chloride mediated activation of glycosyl halide in neutral condition. Tetrahedron *57*, 7701-7704.

Neelamegham, S., and Mahal, L.K. (2016). Multi-level regulation of cellular glycosylation: from genes to transcript to enzyme to structure. Curr Opin Struct Biol *40*, 145-152.

Okayama, M., Kimata, K., and Suzuki, S. (1973). The influence of p-nitrophenyl beta-d-xyloside on the synthesis of proteochondroitin sulfate by slices of embryonic chick cartilage. J Biochem *74*, 1069-1073.

Orth, R., Pitscheider, M., and Sieber, S.A. (2010). Chemical Probes for Labeling of the Bacterial Glucosaminidase NagZ via the Huisgen Cycloaddition. Synthesis-Stuttgart, 2201-2206.

Rillahan, C.D., Antonopoulos, A., Lefort, C.T., Sonon, R., Azadi, P., Ley, K., Dell, A., Haslam, S.M., and Paulson, J.C. (2012). Global metabolic inhibitors of sialyl- and fucosyltransferases remodel the glycome. Nat Chem Biol *8*, 661-668.

Sandhoff, K., and Harzer, K. (2013). Gangliosides and gangliosidoses: principles of molecular and metabolic pathogenesis. J Neurosci *33*, 10195-10208.

Sarkar, A.K., Rostand, K.S., Jain, R.K., Matta, K.L., and Esko, J.D. (1997). Fucosylation of disaccharide precursors of sialyl LewisX inhibit selectin-mediated cell adhesion. J Biol Chem *272*, 25608-25616.

Schworer, R., and Schmidt, R.R. (2002). Efficient sialyltransferase inhibitors based on glycosides of N-acetylglucosamine. J Am Chem Soc *124*, 1632-1637.

Stolfa, G., Mondal, N., Zhu, Y., Yu, X., Buffone, A., Jr., and Neelamegham, S. (2016). Using CRISPR-Cas9 to quantify the contributions of O-glycans, N-glycans and Glycosphingolipids to human leukocyte-endothelium adhesion. Sci Rep *6*, 30392.

Stutz, A.E., and Wrodnigg, T.M. (2016). Carbohydrate-Processing Enzymes of the Lysosome: Diseases Caused by Misfolded Mutants and Sugar Mimetics as Correcting Pharmacological Chaperones. Adv Carbohydr Chem Biochem *73*, 225-302.

Tsuiji, H., Takasaki, S., Sakamoto, M., Irimura, T., and Hirohashi, S. (2003). Aberrant O-glycosylation inhibits stable expression of dysadherin, a carcinoma-associated antigen, and facilitates cell-cell adhesion. Glycobiology *13*, 521-527.

van Wijk, X.M., Lawrence, R., Thijssen, V.L., van den Broek, S.A., Troost, R., van Scherpenzeel, M., Naidu, N., Oosterhof, A., Griffioen, A.W., Lefeber, D.J.*, et al.* (2015). A common sugar-nucleotide-mediated mechanism of inhibition of (glycosamino)glycan biosynthesis, as evidenced by 6F-GalNAc (Ac3). FASEB J *29*, 2993-3002.

Varki, A. (2017). Biological roles of glycans. Glycobiology *27*, 3-49.

Vauzeilles, B., Dausse, B., Palmier, S., and Beau, J.M. (2001). A one-step beta-selective glycosylation of N-acetyl glucosamine and recombinant chitooligosaccharides. Tetrahedron Lett *42*, 7567-7570.

Victor, X.V., Nguyen, T.K., Ethirajan, M., Tran, V.M., Nguyen, K.V., and Kuberan, B. (2009). Investigating the elusive mechanism of glycosaminoglycan biosynthesis. J Biol Chem *284*, 25842-25853.

Wilkins, P.P., McEver, R.P., and Cummings, R.D. (1996). Characterization of the O-glycans of PSGL-1 from HL-60 cells. FASEB J *10*, 1321-1321.

Xue, J., Kumar, V., Khaja, S.D., Chandrasekaran, E.V., Locke, R.D., and Matta, K.L. (2009). Syntheses of fluorine-containing mucin core 2/core 6 structures using novel fluorinated glucosaminyl donors. Tetrahedron *65*, 8325-8335.

Zandberg, W.F., Kumarasamy, J., Pinto, B.M., and Vocadlo, D.J. (2012). Metabolic inhibition of sialyl-Lewis X biosynthesis by 5-thiofucose remodels the cell surface and impairs selectin-mediated cell adhesion. J Biol Chem *287*, 40021-40030.

Zhu, B.C., Drake, R.R., Schweingruber, H., and Laine, R.A. (1995). Inhibition of glycosylation by amphomycin and sugar nucleotide analogs PP36 and PP55 indicates that Haloferax volcanii beta-glucosylates both glycoproteins and glycolipids through lipid-linked sugar intermediates: evidence for three novel glycoproteins and a novel sulfated dihexosyl-archaeol glycolipid. Arch Biochem Biophys *319*, 355-364.

FIGURE LEGENDS

Figure 1. Thio/S- and O-glycosides as metabolic decoys (See also Supplemental data, compound characterization). A. Structures **1**-**6** correspond to S-glycosides. **7**-**12** are O-glycosides. Control molecules, GlcNAc with sulfhydryl group at anomeric position (**13,** 'SH') and GlcNAc (**14**), are also shown. **B-C.** Potential mechanism of S- (panel **B**) and O- (panel **C**) glycoside action as metabolic decoys. In both cases, peracetylated glycosides or decoys are taken up by cells and deacetylated by cellular esterases. These compounds are processed through the Golgi where they form biosynthetic products, including Lewis-X and sialyl Lewis-X type structures. These glycosides divert natural biosynthetic pathways and truncate cell surface glycan biosynthesis. S-glycosides are more effective acceptor-decoys, compared to O-glycosides. Unlike the O-glycosides, they are not spontaneously hydrolyzed by cellular hexosaminidases.

Figure 2. Static selectin-IgG binding and CLA expression altered by O- and S-linked decoys (See also Supplemental Figures S1 and S2). HL60 cells were cultured with 0-100 μM GlcNAc decoys for 40h. Flow cytometry measured the binding of: **A**., **B.** anti-CLA mAb HECA-452, **C., D.** E-selectin-IgG, **E.** L-selectin-IgG, and **F.** P-selectin-IgG to the cells. Dose dependent data for HECA-452 expression and E-selectin-IgG binding are presented in **B**, **D**. Anti-E-selectin (clone P2H3, **B**), L-selectin (Dreg-56, **C**), and P-selectin (G1, **D**) blocking mAbs confirm selectin-IgG binding specificity. NC/Negative-control: secondary antibody alone. IC: isotype control. VC: vehicle control. * $P<0.05$ with respect to VC. S-glycosides reduced E-selectin IgG binding and CLA expression more dramatically compared to the O-glycosides. All S-glycosides, except **4**, also partially reduced L-selectin IgG binding. **1** (SNAP), **7** (ONAP) and **13** (SH) are indicated in the different panels as they are the focus of subsequent studies.

Figure 3. Effect of SNAP on cell adhesion under flow. HL60s were cultured with SNAP, ONAP, SH or VC (0.2% DMSO) for 40h. Cells were then perfused at wall shear stress of 1 dyne/cm^2 over substrates bearing: **A, E.** IL-1β stimulated HUVEC monolayers, **B, F.** recombinant human E-selectin IgG, **C, G.** L-selectin IgG, or **D, H.** P-selectin IgG. Interacting cells were classified into rolling or firmly adherent cells (top panels). Cell rolling velocity was also recorded in the cumulative line plots (bottom panels). Blocking

antibodies used were against E-selectin (P2H3), L-selectin (Dreg-56) or PSGL-1 (KPL-1). SNAP increased cell rolling velocity on stimulated HUVECs, E-selectin IgG and L-selectin IgG substrates, as indicated by red median velocity markings in panels E-G. *P<0.05 for total interacting cells with respect to VC, SNAP, ONAP and SH, except as indicated in panel A.

Figure 4 Murine model of acute inflammation. A. Bone marrow cells (mBMCs) were collected from 10-12 week old WT C57BL/6 mice. These were cultured with 100 μM ONAP, SNAP or 0.25% DMSO (VC) for 40 h *ex vivo*, differentially labeled with fluorescence reporters, mixed in approximately equal proportion, and then injected into recipient mice. Peritonitis was induced 1h before injection. Twenty hours later, samples from the peritoneal lavage and bone marrow were collected and analyzed using cytometry. **B.** In 'Mix 1', ONAP, SNAP, and VC treated cells were labeled with either green, red or green+red dyes, respectively. The dyes were swapped in 'Mix 2' and 'Mix 3'. Panel presents raw cytometry data showing distinct labeled cell populations at the top-left, bottom-right and top-right quadrants. Reduced cell numbers upon SNAP treatment are indicated by blue arrows. **C-D.** In both the peritoneum (panel C) and bone marrow (D), the number of labeled 1A8/Gr-1+ cells was reduced dramatically (>90%) in the case of SNAP treatment compared to either ONAP or VC. * P<0.05 between indicated treatments.

Figure 5. Truncation of O-glycan biosynthesis by SNAP (See also Supplemental Figures S3-S5). A-D. Wild-type HL-60s were cultured with 80 μM ONAP, SNAP or vehicle controls for 40 h. Flow cytometry measured cell surface carbohydrate structures using either fluorescent antibodies or lectins: PNA (binds Galβ1,3GalNAc, panel **A**), ECL (binds Galβ1,4GlcNAc, **B**), PHA-L (binds complex N-glycans, **C**), and CD15/Lewis-X (mAb HI98, **D**). Data in inset are mean fluorescence intensity ± SD for >3 independent experiments. * P<0.05 with respect to VC. SNAP increased PNA, ECL, and PHA-L bindings. ONAP has a smaller effect. **E-F.** Cell lysates run under standard reducing conditions, were probed with mAbs against mucinous proteins, anti-human PSGL-1 mAb TB5 (panel **E**) and anti-human CD43 mAb L60 (**F**). SNAP reduced molecular mass of both glycoproteins indicating truncation on O-glycans. **G.** HL-60s were treated with 80 μM glycosides or vehicle control. Cell lysates were incubated with 10,000 dpm UDP-[^{14}C]Gal (donor)

in the presence or absence of 0.5 mM GalNAc-OBn (acceptor). [^{14}C]Gal is preferentially added to SNAP present in cell lysates rather than GalNAc-OBn (left-half). Even in the absence of GalNAc-OBn, radioactive products are formed on SNAP and ONAP (right-half). **H-J.** HL-60s were cultured with 80 μM ONAP, SNAP or GalNAc, with 100 μM GalNAc-OBn being added after 8h in some cases. Products secreted into culture medium over 2 days were collected and quantitatively analyzed using LC-MS/MS. SNAP, and to a lesser extent ONAP, reduces glycan biosynthesis on GalNAc-OBn (panel **H**). Extended carbohydrate chains grew on SNAP (panel **I**) and ONAP (**J**). All assignments were verified by MS/MS. *P<0.05, **P<0.01 with respect to GalNAc. †: No detected.

Figure 6. Whole cell glycomics profiling following SNAP treatment: A-B. N-linked glycans, **C.** glycosphingolipids and **D.** O-linked glycans isolated from HL60 cells that were cultured with 60 μM of vehicle control (upper panels) or SNAP (lower panels). **B**. MALDI-TOF MS spectra of N-glycans of the zoomed scan *m/z* 3134 to 3155 and of *m/z* 3945 to 3964 molecular ion clusters derived either from vehicle control (upper panels) or SNAP (lower panels) of **A**. Red peaks on SNAP treated N-linked glycans and glycosphingolipids spectra correspond to GlcNAc terminated (agalactosylated) structures that appear upon SNAP treatment. Isolated glycans were permethylated and analyzed by MALDI-TOF MS. All molecular ions are $[M+Na]^+$. Putative structures are based on composition, tandem MS and biosynthetic knowledge. Structures that show sugars outside a bracket have not been unequivocally defined.

Figure 7. Hydrolysis of O-glycosides in cells (See also Supplemental Figure S7). A.-D. HL60s were cultured with 80 μM SNAP, ONAP or vehicle control. After 40 h, the medium was extracted and analyzed using HPLC (224nm detection). Standards were created by spiking culture media with 2-naphthalenemethanol (HONAP) and 2-naphthalenemethanethiol (HSNAP) standards at 1:1 ratio (panel **A**). These compounds eluted at 17 and 29 min, respectively. Media with vehicle control had no peaks (panel **B**). Peak corresponding to HONAP retention time was seen in supernatants from cells cultured with ONAP (black arrowhead, **C**). Cells cultured with SNAP did not have product corresponding to HSNAP (**D**). **E-G.** HONAP was derivatized by dansyl chloride to serve as a MS standard (chemical reaction in schematic).

No peak was observed in vehicle control (panel **E**). Dansyl derivatization was performed for products extracted from cell culture medium in runs with ONAP, SNAP and VC. Dansylated HONAP was only observed in runs with ONAP (panel **G**) and this was verified by MS/MS (with respect to synthetic standard in panel **F**). The equivalent product was not observed in cells cultured with SNAP or vehicle. Thus, ONAP, but not SNAP, was hydrolyzed within cells. **H.-I.** Cells were co-treated with a mix of 80 µM SNAP together with ONAP for 40 h. Glycosylated products formed on ONAP and SNAP present in supernatant (panel **H**) and cell pellet (**I**) were analyzed using LC-MS/MS. Larger glycan products were formed on SNAP compared to ONAP. 'NAPX' is used to denote both O- and S-glycosides. All structures were verified by MS/MS. **P*<0.05, ***P*<0.01, ****P*<0.01 with respect to ONAP. † Not detected.

STAR Methods

CONTACT FOR REAGENTS AND RESOURCE SHARING

Further information and requests for resources and reagents should be directed to and will be fulfilled by the Lead Contact, Sriram Neelamegham (neel@buffalo.edu). Chemical compounds will be provided via TumorEnd LLC.

EXPERIMENTAL MODEL AND SUBJECT DETAILS

10-12 week-old C57BL/6 wild-type mice of either sex were used. Animals were randomized prior to experimentation. All animal studies were approved by the Roswell Park Cancer Institute Animal Care and Use Committee (RPCI-IACUC). HL-60 cells (female promyeloblasts, RRID:CVCL_0002), T47D (female ductal carcinoma, RRID: CVCL_0553) and ZR-75-1 (female epithelial ductal carcinoma, RRID: CVCL_0588), and metastatic prostate PC-3 cells (male adenocarcinoma, RRID: CVCL_0035) were obtained from ATCC. Human Umbilical Vein Endothelial Cells (HUVECs, cat #CC-2519A) were from Lonza.

METHODS DETAILS

Chemical synthesis

The synthesis of GlcNAc derivatives is described below. These include a series of thio/S-glycosides: peracetylated GlcNAc-β-S-NAP (**1**, abbreviated 'SNAP'), GlcNAc-β-S-NAP (**2**), peracetylated GlcNAc-β-S-geranyl (**3**), GlcNAc-β-S-geranyl (**4**), peracetylated GlcNAc-β-S-bromooctane (**5**) and peracetylated GlcNAc-β-S-benzyl (**6**). The O-glycosides include peracetylated GlcNAc-β-O-NAP (**7**, abbreviated 'ONAP'), GlcNAc-β-O-NAP (**8**), peracetylated GlcNAc-β-O-methoxyphenyl (**9**), GlcNAc-β-O-methoxyphenyl (**10**), GlcNAc-β-O-geranyl (**11**) and GlcNAc-β-O-benzyl (**12**). Control molecules used are peracetylated GlcNAc-β-SH (**13**, abbreviated 'SH'); and GlcNAc (**14**).

GlcNAcβZ (*O*-glycosides) synthesis [footnote-1]: 2-Acetamido-2-deoxy-D-glucopyranose (1.77 g, 8.0 mmol) was suspended in acetyl chloride (AcCl, 8 mL) at 0°C under nitrogen and the mixture was stirred at room temperature (r.t.) overnight (Horton and Wolfrom, 1962; Orth et al., 2010). The solvent was removed under vacuum, then the residue was diluted with dichloromethane (15 -25 mL) and extracted with ice water until the pH value of the aqueous layer was neutral. The organic layer was dried and concentrated. The 2-acetamido-3,4,6-tri-*O*-acetyl-2-deoxy glucopyranosyl chloride obtained was a colorless solid. In the second step, the chloride (365 mg, 1.0 mmol) was stirred with 2-naphthalenemethanol (158 mg, 1.0 mmol), and freshly prepared molecular sieves 4Å (500 mg) in CH_2Cl_2 (8 mL) for 6-8 h. To this mixture, $InCl_3$ (110 mg, 0.5 mmol) was added and the reaction was stirred for additional 16-20 h at room temperature (Mukherjee et al., 2001). The progress of the formation of the product was examined by TLC (ethylacetate/hexane 1:1 or dichloromethane/acetone 4:1). The reaction mixture was then diluted with CH_2Cl_2 (8 mL), filtered over celite and washed with saturated sodium bicarbonate solution (3 times), and dried over Na_2SO_4. It was filtered and concentrated *in vacuo*. The desired product was purified using silica gel flash chromatography using solvent gradients ethylacetate/hexane 1:2 or acetone/dichloromethane 1:10. In most cases, compounds were obtained as solid materials. 2-naphthalenemethanol was replaced by other aglycon alcohols to obtain other *O*-glycosides, except for **9** & **10**. Detailed reaction scheme is shown below.

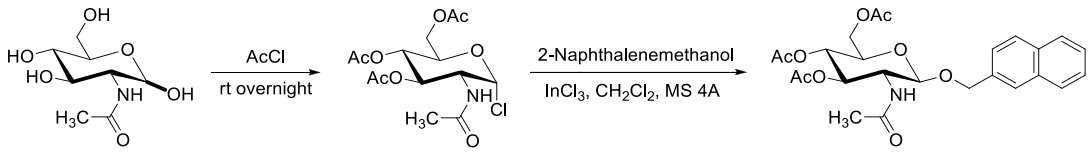

Synthesis of acetylated GlcNAcβSZ: For preparation of thiourea salt (Horton and Wolfrom, 1962; Ibatullin et al., 2001), thiourea (3.8 g, 5 mmol) was added to a mixture of 2-acetamido-3,4,6-tri-*O*-acetyl-2-deoxy glucopyranosyl chloride (1.83 g, 5 mmol) in acetonitrile (10 mL). The reaction was refluxed for 10 min. Then the solvent was evaporated. After crystallization from acetone, product was obtained as white solid. In the next step, 2-(bromomethyl)naphthalene (442 mg, 2 mmol) was added to a solution of thiourea salt (885 mg, 2 mmol) in acetonitrile (10 mL), followed by TEA (0.7 mL, 5 mmol) (Ibatullin et al., 2001). The reaction was

Footnote-1 **PTC patent WO/2016/077567** "*Compositions, Methods, and Treatments for Inhibiting Cell Adhesion and Virus Binding and Penetration*" Matta, K. L.

stirred at r.t. for 1 day, and then concentrated *in vacuo*. The crude product was purified by flash chromatography using acetone /dichloromethane which afforded a white solid product.

In an alternate method reported earlier (Matta et al., 1973), the urea salt treated with potassium pyrosulfite in refluxing mixture of water and chloroform gave 2-acetamido-3,4,6-tri-*O*-acetyl-2-deoxy-1-thio-β-glycopyranose **13** (Matta et al., 1973). The latter on treatment with alkyl bromide in acetone in the presence of anhydrous potassium carbonate in acetone (Claeyssens et al., 1970) can give alkyl-thio glycosides. 2-(bromomethyl)naphthalene was replaced by other aglycone halides (Z-halide) in the above reaction to furnish the remaining acetylated GlcNAcβSZ compounds from **13**. The full reaction scheme is shown below.

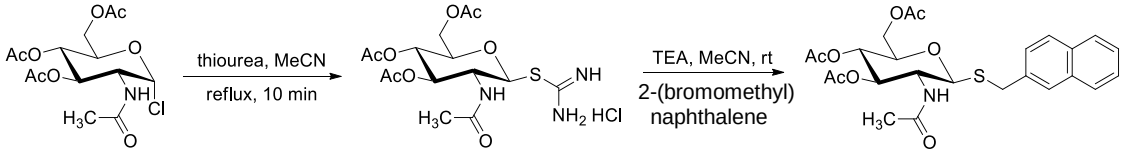

Synthesis procedure for *p*-methoxyphenyl 2-acetamido-3,4,6-tri-*O*-acetyl-2-deoxy-β-D-glucopyranoside **9:** To a solution of β-D-glucosamine pentaacetate (10 g, 25 mmol) and *p*-methoxyphenol (9.5 g, 75 mmol) in CH_2Cl_2 (180 mL) chilled in salt ice bath, was added $BF_3{\cdot}OEt_2$ (4.7 mL, 37.5 mmol) dropwise (Fettke et al., 2009). The reaction was stirred at room temperature for 24 h, and then was washed with water, $NaHCO_3$ solution, and brine. The organic layer was dried ($MgSO_4$) and concentrated. The residue was purified with flash chromatography which afforded product as white solid. Compound **10** was obtained by deacetylation of **9**.

De-*O*-acetylation: Thio and *O*-glycosides were deacetylated using sodium methoxide in methanol. Typically, to a solution of 1 mmol starting material in MeOH (10 mL), 5-10 drops NaOMe/MeOH 0.5 M solution was added. The reaction was allowed to stir for overnight. When reaction was complete, the solution was filtered through a short pack of Dowex 50W resin, and concentrated. The resulted white solid was washed with small amount of cold MeOH and filtered.

For large scale preparation of GlcNAc-βONAP has already been reported from Matta's group (Xue et al., 2009) wherein one-step β-selective glycosylation of *N*-acetylglucosamine (Vauzeilles et al., 2001)

with NAP-bromide in presence of lithium bromide and sodium hydride was found to be effective in providing the target compound as solid material.

Cell culture and chemical treatment

All cell lines were cultured according to ATCC (Manassas, VA), unless otherwise mentioned. HUVECs were cultured in EBM-2 media (Lonza). Isogenic HL-60 clones lacking extended O-glycans ($[O]^{-}$ cells), N-glycans ($[N]^{-}$) and glycolipids ($[G]^{-}$) were available from a previous study (Stolfa et al., 2016). These cells lack the genes COSMC (core-1 β3 galatoctosyltransferase molecular chaperone), MGAT1 (mannosyl α1,3-glycoprotein β1,2-*N*-acetylglucosaminyltransferase) and UGCG (UDP-Glucose Ceramide Glucosyltransferase), respectively.

For cell treatment, all GlcNAc-based glycosides were dissolved in DMSO to make 40 mM stocks, and stored at -20°C until use. In typical runs, the GlcNAc O- and S-glycosides were added to 0.5-1×10^6 cells/mL at 0-200 μM in normal culture medium for 2-days (~40 h). All runs included control compounds (**13**, **14**) and/or vehicle control (typically 0.2-0.25% DMSO). In some runs, HL-60s were differentiated to terminal neutrophils by culturing cells with 1.3% DMSO over 5 days (Marathe et al., 2008). Here, on day-3, 80 μM SNAP, ONAP, SH or 0.2% DMSO (vehicle) was added to the culture medium. Cells analysis was performed on day-5. In other cases, 100 μM peracetylated α-benzyl GalNAc (abbreviated 'GalNAc-O-Bn'), available from a previous study (Stolfa et al., 2016), was added along with ONAP or SNAP for subsequent MS analysis. In each case, at the treatment end-point, the cells were harvested and resuspended in HEPES buffers (30 mM HEPES, 110 mM NaCl, 10 mM KCl, 2 mM $MgCl_2$, 10 mM glucose, pH 7.3) containing 0.1% HSA (human serum albumin) and 1.5 mM Ca^{2+}. Cell surface glycan analysis and functional assays were then performed using flow cytometry, microfluidics based cell adhesion assays, Western blotting and enzymology as described previously ((Buffone et al., 2013; Marathe et al., 2008; Mondal et al., 2015), see below).

Antibodies and lectins

Antibodies employed for cytometry analysis include fluorescent rat anti-Cutaneous Lymphocyte Antigen/CLA mAb HECA-452 (IgM) which recognized sialyl Lewis-X/sLe^X and related antigens, mouse anti-human CD11b mAb D12 (IgG), mouse anti-CD15/Lewis-X mAb HI98 (IgM), and isotype controls. Function blocking mAbs used include anti-human PSGL-1 mAb KPL-1, anti-P-selectin mAb G1, anti-E-selectin mAb P2H3, and anti-L-selectin mAb DREG-56. Lectins used in this study include fluorescein-conjugated Peanut agglutinin (PNA; binds the T-antigen or Galβ1,3GalNAc), *Erythrina cristagalli* lectin (ECL; binds *N*-acetyl lactosamine Galβ1,4GlcNAc), *Phaseolus vulgaris Leucoagglutinin* (PHA-L; binds Galβ4GlcNAcβ6(GlcNAcβ2Manα3)Manα3 on N-glycans), and biotinylated *Maackia amurensis lectin II* (MAL-II; binds α(2,3) linked sialic acid). Recombinant human L-/CD62L, E-/CD62E and P-/CD62P selectin IgG fusion proteins were also used.

Flow cytometry

Typically, cells suspended in HEPES buffer with 0.1% HSA (human serum albumin) and 1.5 mM Ca^{2+} were incubated with 1-10 μg/mL of fluorescent monoclonal antibodies or lectins for 20 min on ice prior to flow cytometry analysis using either a FACSCalibur or LSRFortessa X-20 instrument (BD Biosciences). In the case of MAL-II binding measurements, FITC-conjugated anti-biotin Ab was also added in a second incubation step as this lectin was biotinylated. For static selectin binding assays, 3 μg/mL human selectin-IgG was first complexed with 10 μg/mL PerCP-conjugated anti-human Fc Ab (Jackson ImmunoResearch, West Grove, PA) in HEPES buffer containing 1% goat serum and 1.5 mM Ca^{2+} for 10 min at r.t.. In some cases, 5-10 μg/mL anti-selectin blocking mAbs were also added in this step. The selectin-PerCP Ab complex was then incubated with 1×10^6 HL-60 cells/mL for 10 min at r.t., prior to 10-fold dilution of the mixture in HEPES buffer (with 0.1% HSA and 1.5 mM Ca^{2+}) and cytometry analysis.

Microfluidics based leukocyte adhesion assay

Cell adhesion studies were performed as described previously (Buffone et al., 2013), using a 100 μm × 400 μm cross-section custom microfluidic flow cell placed on the stage of a Zeiss AxioObserver Z1 microscope.

Here, the flow cell substrate was composed of either 4 h IL-1β stimulated HUVEC monolayers, or recombinant L-, E- or P-selectin IgG at physiological levels (Mondal et al., 2015). Control or glycoside treated HL-60s at 2×10^6 cells/mL resuspended in HEPES buffer contained 1.5 mM Ca^{2+} and 0.1% HSA were perfused over these substrates at a wall shear stress of 1 dyn/cm^2. Cell rolling density, firm adhesion density and cell rolling velocity was measured as described previously. Ten μg/mL function blocking mAbs were applied in some cases to block the function of either the immobilized selectins on the flow cell substrate or the selectin-ligand PSGL-1 on the leukocytes.

Western blot analysis

HL-60 cells were cultured with 80 μM SNAP, ONAP, SH or 0.2% DMSO (vehicle). These cells were washed and resuspended in 90 μL Laemmli sample buffer (Bio-rad) containing β-mercaptoethanol. After denature by boiling at 95 °C for 5 min, debris was pelleted by centrifugation. 20 μL supernatant was resolved using 4-20% gradient SDS-PAGE. Next, the proteins were transfer onto 0.2 μm nitrocellulose membrane, and probed with either anti-human PSGL-1 mAb TB5 (GeneTex, Irvine, CA) or anti-human CD43 mAb L60 (BD Biosciences). A secondary horse-radish peroxidase (HRP) coupled anti-mouse Ab was incubated with the membrane prior to chemiluminescence development using ECL substrate (Thermo-Pierce).

Galactosyltransferase assay

10^7 HL-60 cells with different treatments (80μM SNAP, ONAP, SH, or 0.2% DMSO) were lysed using either RIPA buffer or sonication (3 cycles of 10s on and 10s off, 40% amplitude), both in the presence of Halt™ protease inhibitor (Thermo). The cell debris was pelleted by centrifugation at 18,000 g for 15 min, and the supernatant was collected. In some runs, a 25 μL reaction was prepared with 60 μg lysate-supernatant and 10,000 dpm UDP-[C^{14}]Gal (258.00 mCi/mmol uridine di-phosphate-galactose, PerkinElmer, Boston, MA) in reaction buffer (100 mM HEPES, 7 mM ATP, 20 mM manganese acetate), either with or without the substrate 0.5 mM GalNAc-O-Bn (de-acetylated). Following overnight reaction, 1 μL reaction mixture spots were placed on thin layer chromatography/TLC plates (Selecto Scientific, Suwanee, GA). Radioactive product was resolved from unreacted C-14 nucleotide-sugar using $CHCl_3$:CH_3OH:H_2O (5:4:1) solvent, and

TLC image was recorded using a Storm 860 phosphorimager (GE Healthcare). In other runs, 60 µg of vehicle-treated lysate was mixed with 500 µM ONAP/SNAP substrate and 1 mM UDP-Gal in reaction buffer in the same reaction buffer (25 µL volume). Following overnight reaction, proteins were precipitated by addition of 1 mL 70% acetonitrile and vortexing. Supernatant collected following centrifugation (14,000 g x 5 min) was evaporated under high vacuum, resuspended in 50 µL 50% MeOH and injected into LC-MS (T*hermo* Scientific™ Q Exactive™ Hybrid Quadrupole-Orbitrap Mass Spectrometer) using C18 separation.

ppGalNAcT assay

The enzymatic reaction was performed in 20 µL reaction buffer (100 mM HEPES, 7 mM ATP, 20 mM manganese acetate, Halt™ protease inhibitor) containing 60 µg lysate-supernatant, 50,000 dpm UDP-[C^{14}]GalNAc (55 mCi/mmol, ARC Inc., St. Louis, MO) and 50 µg PSGL-1 *N*-terminal peptide substrate (AQTTPRAATEAQTTRLRATESHHHHHH, GenScript, Piscataway, NJ). Following overnight reaction at r.t., reaction volume was increased 10-fold using 500 mM NaCl in phosphate-buffered saline (PBS) and mixed with 10 µL MagneHis™ Ni-Particles (Promega, Madison, WI) for 45 min at r.t.. Followed 5-wash cycles in washing buffer (100 mM NaCl, 10 mM imidazole in PBS) using magnetic separation at each step, the entire mixture was brought up to 200 µl in the washing buffer and mixed with 4mL scintillation cocktail. The UDP-[C^{14}]GalNAc radioactivity associated with the peptide immobilized with the beads was quantified using a standard scintillation counter.

Animal studies

Mouse bone marrow cells (mBMCs) were isolated from the tibia and femur of 10-12 week old C57BL/6 donor mice. These mBMCs were cultured *ex vivo*, with 100 µM ONAP, SNAP or vehicle (0.25% DMSO) in IMDM media containing 10 ng/mL G-CSF, 1 ng/mL IL-3 and 10% FBS. Following culture for 40 h, the cells were labeled using the green fluorescent dye CMFDA (1 µM) (Setareh Biotech, Eugene, OR), orange dye CMTMR (5 µM) or both dyes together by incubating the dye with the cells for 15 min at 37°C. The exact dye used for individual cell types was varied to ensure that dye labeling did not influence the study findings. Following this, the three labeled cell types were mixed in approximately equal amounts and infused *i.v.* into

recipient mouse injected with 4% thioglycollate *i.p.* to induce peritonitis (Marathe et al., 2010). Samples from the peritoneal lavage and bone marrow were collected 20h thereafter. Granulocytes in the collected samples were identified based on their characteristic forward-side scatter profile, and labeling with APC conjugated anti-mouse Ly-6G clone 1A8 (BioLegend, San Diego, CA). Granulocytes tagged with green and/or red fluorescent dyes were enumerated using a BD LSR-II flow cytometer. Final data are normalized with respect to the cell ratio in the injected mixture.

MALDI TOF MS/MS glycomics profiling

N-linked, O-linked and GSL derived glycans were extracted from vehicle control and SNAP treated HL60s as described previously (Mondal et al., 2015). All glycans were permethylated prior to MALDI-TOF MS and MALDI-TOF-TOF MS/MS analysis. Released glycans from GSLs were deuteroreduced prior to permethylation. Data were annotated using the glycobioinformatics tool, GlycoWorkBench (Ceroni et al., 2008). The proposed assignments for the selected peaks were based on ^{12}C isotopic composition together with knowledge of the biosynthetic pathways. The proposed structures were confirmed using MS/MS.

LC-MS/MS glycan analysis

HL-60s (0.3×10^6/mL) were cultured for 48 h in advance-DMEM without phenol red (ADMEM). In some cases, 60-100μM SNAP, ONAP, or peracetylated benzyl-α-GalNAc was added alone to the culture medium, while in other cases two compounds were mixed and added together. 0.2% DMSO served as vehicle. Cell culture medium was purified using Sep-Pak C18 columns (Waters, Milford, MA), with glycosides being released by elution with 50-75% MeOH. The released product was permethylated prior to MS analysis (Stolfa et al., 2016). In some cases, to examine glycans formed within cells, cell pellets were collected in the above runs, and lysed using 75% MeOH followed by sonication. Following removal of cell debris by centrifugation at 18,000 g for 15 min, the supernatant was dried using a CentriVap centrifugal evaporator. Three mL ADMEM was added to resuspend the glycans. Separation using C18 Sep-Pak and permethylation was performed as above.

For LC-MS analysis, the above samples were filtered through 0.2 µm PES (Polyethersulfone) syringe filters, centrifuged at 16,000 g at 4 °C for 15 min to remove any debris, and the supernatant was analyzed. Two instruments were used: i. An Orbitrap-XL MS (Thermo) equipped with a nano-LC column (PepMap C18 2 µm; 75 µm×150 mm, Thermo) and ESI (electrospray ionization) source; ii. A 6530 Accurate Mass Dual Agilent Jet Stream ESI-Q-ToF (quadrupole-time-of-flight) with a Phenomenex Gemini C18 column (5 µm, 4.6 x 50 mm). In the Orbitrap-XL runs, the mobile phases were, A: water and B: acetonitrile (CH_3CN), both containing 0.1% (v/v) formic acid. Data were acquired over 80 min at a flow rate of 300 nL/min using the following linear gradient: (i) increase from 0% to 20% B (0-5 min); (ii) 20% to 40% B (5-45 min); (iii) 40% to 70% B (45-65 min); (iv) 70% to 100% B (65-75 min); and (v) isocratic elution at 100% B (75-80 min). MS^1 data were acquired using the Orbitrap detector (60,000 resolution), and MS/MS in CID mode (ion trap with 30% collision energy). For ESI-Q-ToF separation, the mobile phases were, A: 10% CH_3CN and B: 90% CH_3CN, both with 0.1% formic acid and 0.1% ammonium formate. Flow rate was set to 0.5 mL/min. MS analysis started at isocratic 100% A (0-5 min), linear ramp to 100% B (5-40 min) and finally isocratic 100% B (40-50 min). MS data were collected over 50-1700 *m/z* in positive ESI mode at high resolution. Targeted LC-MS/MS analyses were carried out by varying collision energies from 0-75 eV. Data were annotated using the glycoinformatics tools DrawGlycan-SNFG (Cheng et al., 2017).

2-Napthalenemethanol detection and analysis

In a variation of the Folch method (Folch et al., 1957), 1.8 mL of HL-60 culture media was transferred to a glass vial and mixed with methanol and chloroform in a ratio 3:4:8 (media:methanol:chloroform). The mixture was vortexed for 1 min and allowed to settle for 1 min, with this vortex-settling cycle being repeated thrice. In the final step, the sample was centrifuged at 500 g for 10 min, and 4.4 mL of the chloroform layer was collected and vacuum-dried.

In one experiment, this product was resuspended in 500 µL MeOH and resolved using an Agilent 1100 HPLC equipped with a reversed-phase ZORBAX Eclipse XDB-C18 column (5 µm, 4.6 mm × 150 mm). Mobile phase A: water and B: methanol, both containing 0.1% (v/v) formic acid. Flow rate was 0.5 mL/min and detector wavelength was 224 nm. Data were acquired over 40 min using the following gradient: (i)

isocratic at 40% B (0-3 min), (ii) increase from 40% to 70% B (3-13 min); (iii) isocratic 70% B (13-23 min); (iv) increases from 70% to 85% B (23-25 min); (v) isocratic 85% B (25-35 min), (vi) decrease from 85% to 40% B (35-37 min), and finally (vii) isocratic 40% B (37-40 min). Pure 2-naphthalenemethanol and 2-napthalenemethanethiol (Sigma) added to culture media served as standards for this run. Calibration curves were linear over the 5–150 µM range for HONAP (r^2 = 0.9997) and HSNAP (r^2 = 0.9985). The limits of detection (LoD) and quantification (LoQ) were 3.8 µM and 11.4 µM for HONAP and 9.1 µM and 27.6 µM for HONAP. Quantifications were carried out in triplicates.

In another experiment, dansyl derivatization was performed by resuspending the above vacuum-dried sample with 100 µL of an amine mixture (0.4% v/v triethylamine or TEA and 6 mg/mL 4-dimethylaminopyridine or DMAP). After vortexing for 1 min, 100 µL of dansyl chloride (6 mg/mL) were added and the reaction was stirring at 600 rpm for 1 h at r.t. in dark. The solvent and triethylamine were then eliminated under high vacuum and the residue was resuspended in 750 µL MeOH. This sample was injected into an LC-ESI-Q-ToF system (Agilent) using LC and MS parameters listed in the previous section. 2- Napthalenemethanol was dansyl derivatized to serve as MS standard.

QUANTIFICATION AND STATISTICAL ANALYSIS

All data are presented as Mean ± S.D ($n \geq 3$). Individual data points are plotted in each panel to give a measure of *n* in each group/condition. Two-tailed Student's T-test was used for dual-comparisons. Analysis of variance (ANOVA) followed by the Student-Newman-Keuls post-test was used for multiple comparisons. $P<0.05$ was considered to be statistically significant.

DATA AND SOFTWARE AVAILABILITY

Two software are used to annotate MS spectra: GlycoWorkBench and DrawGlycan-SNFG. Both resources are provided open-source at github (see key resources table).

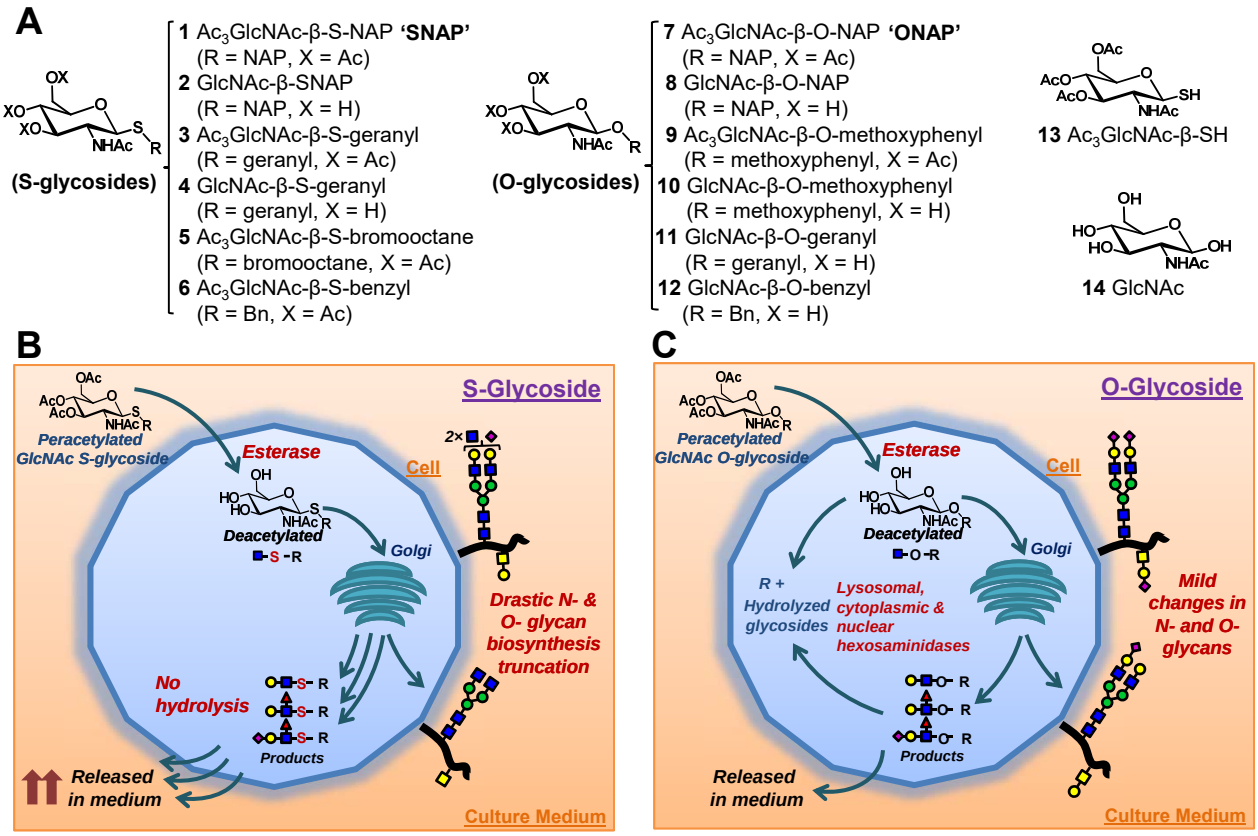
A
(S-glycosides)
1 Ac3GlcNAc-β-S-NAP 'SNAP'
(R = NAP, X = Ac)
2 GlcNAc-β-SNAP
(R = NAP, X = H)
3 Ac3GlcNAc-β-S-geranyl
(R = geranyl, X = Ac)
4 GlcNAc-β-S-geranyl
(R = geranyl, X = H)
5 Ac3GlcNAc-β-S-bromooctane
(R = bromooctane, X = Ac)
6 Ac3GlcNAc-β-S-benzyl
(R = Bn, X = Ac)
(O-glycosides)
7 Ac3GlcNAc-β-O-NAP 'ONAP'
(R = NAP, X = Ac)
8 GlcNAc-β-O-NAP
(R = NAP, X = H)
9 Ac3GlcNAc-β-O-methoxyphenyl
(R = methoxyphenyl, X = Ac)
10 GlcNAc-β-O-methoxyphenyl
(R = methoxyphenyl, X = H)
11 GlcNAc-β-O-geranyl
(R = geranyl, X = H)
12 GlcNAc-β-O-benzyl
(R = Bn, X = H)
13 Ac3GlcNAc-β-SH
14 GlcNAc
B
S-Glycoside
Peracetylated GlcNAc S-glycoside
Esterase
Deacetylated
Cell
Golgi
2×
Drastic N- & O- glycan biosynthesis truncation
No hydrolysis
Products
Released in medium
Culture Medium
C
O-Glycoside
Peracetylated GlcNAc O-glycoside
Esterase
Deacetylated
Cell
Golgi
R + Hydrolyzed glycosides
Lysosomal, cytoplasmic & nuclear hexosaminidases
Mild changes in N- and O- glycans
Products
Released in medium
Culture Medium

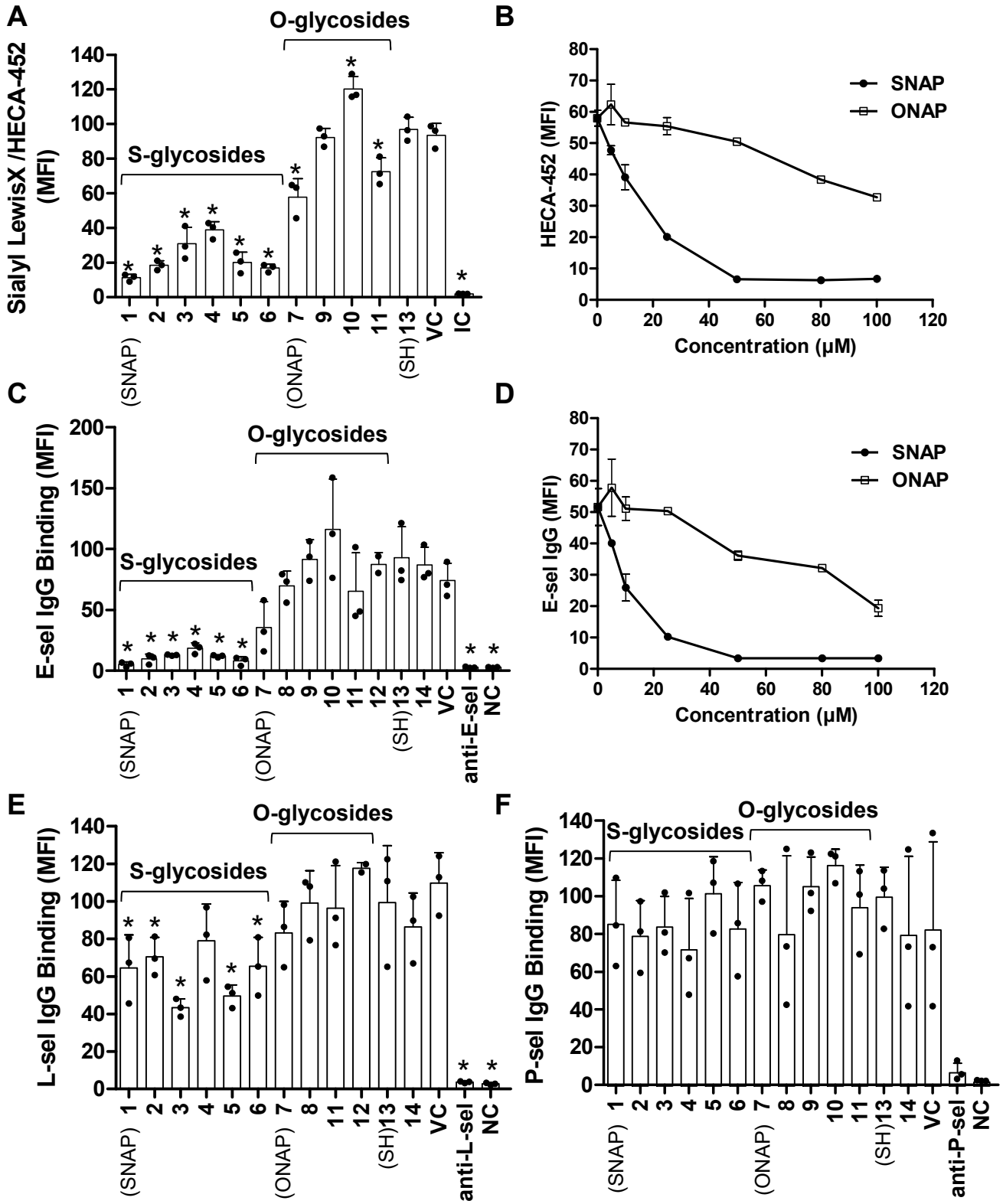
A
Sialyl LewisX /HECA-452 (MFI)
O-glycosides
S-glycosides
1 2 3 4 5 6 7 9 10 11 13 VC IC
(SNAP) (ONAP) (SH)
B
HECA-452 (MFI)
SNAP
ONAP
Concentration (μM)
C
E-sel IgG Binding (MFI)
O-glycosides
S-glycosides
1 2 3 4 5 6 7 8 9 10 11 12 13 14 VC anti-E-sel NC
(SNAP) (ONAP) (SH)
D
E-sel IgG (MFI)
SNAP
ONAP
Concentration (μM)
E
L-sel IgG Binding (MFI)
O-glycosides
S-glycosides
1 2 3 4 5 6 7 8 11 12 13 14 VC anti-L-sel NC
(SNAP) (ONAP) (SH)
F
P-sel IgG Binding (MFI)
O-glycosides
S-glycosides
1 2 3 4 5 6 7 8 9 10 11 13 14 VC anti-P-sel NC
(SNAP) (ONAP) (SH)

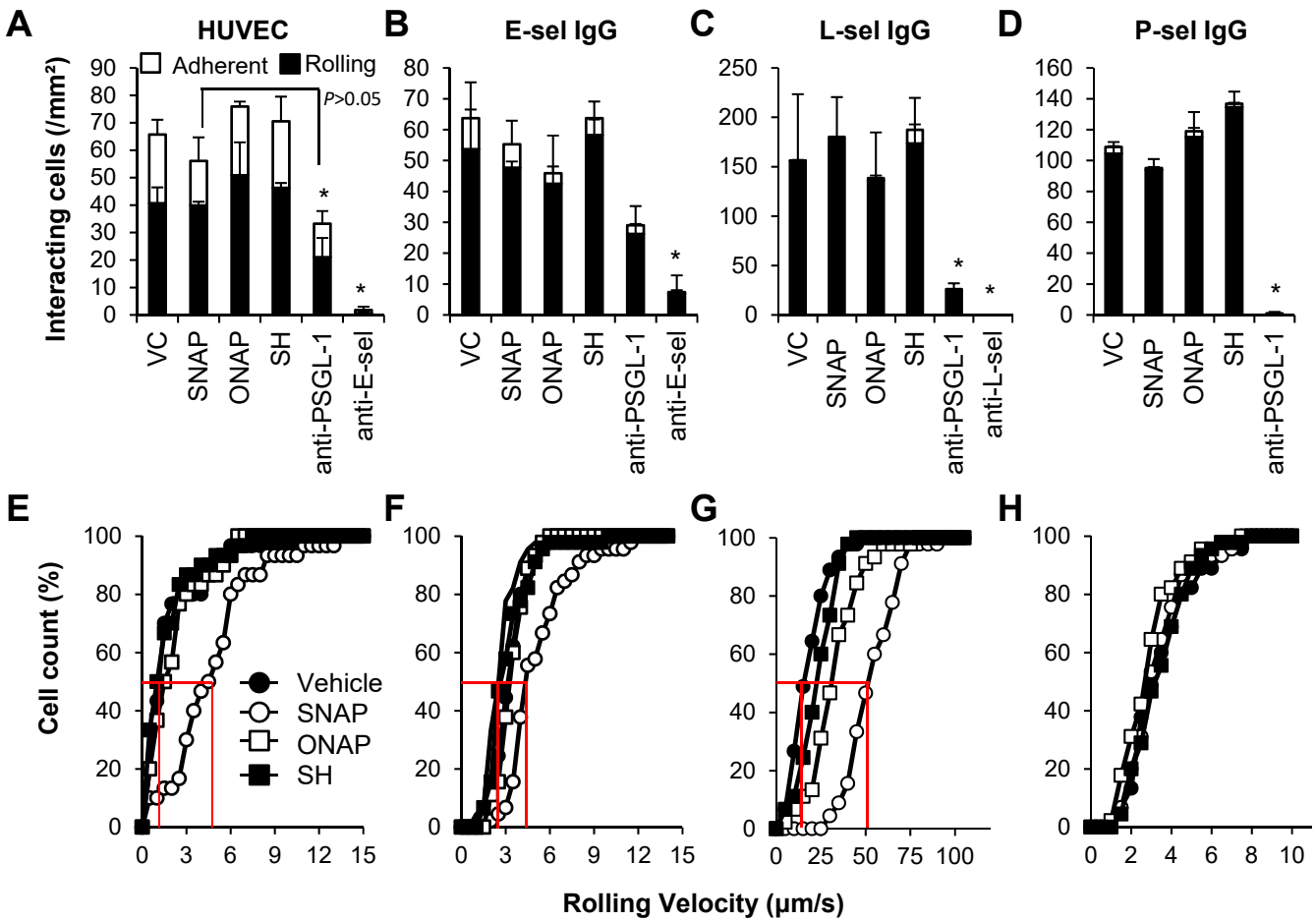
A
HUVEC
Adherent
Rolling
P>0.05
Interacting cells (/mm²)
VC
SNAP
ONAP
SH
anti-PSGL-1
anti-E-sel
B
E-sel IgG
C
L-sel IgG
anti-L-sel
D
P-sel IgG
E
F
G
H
Cell count (%)
Vehicle
SNAP
ONAP
SH
Rolling Velocity (μm/s)

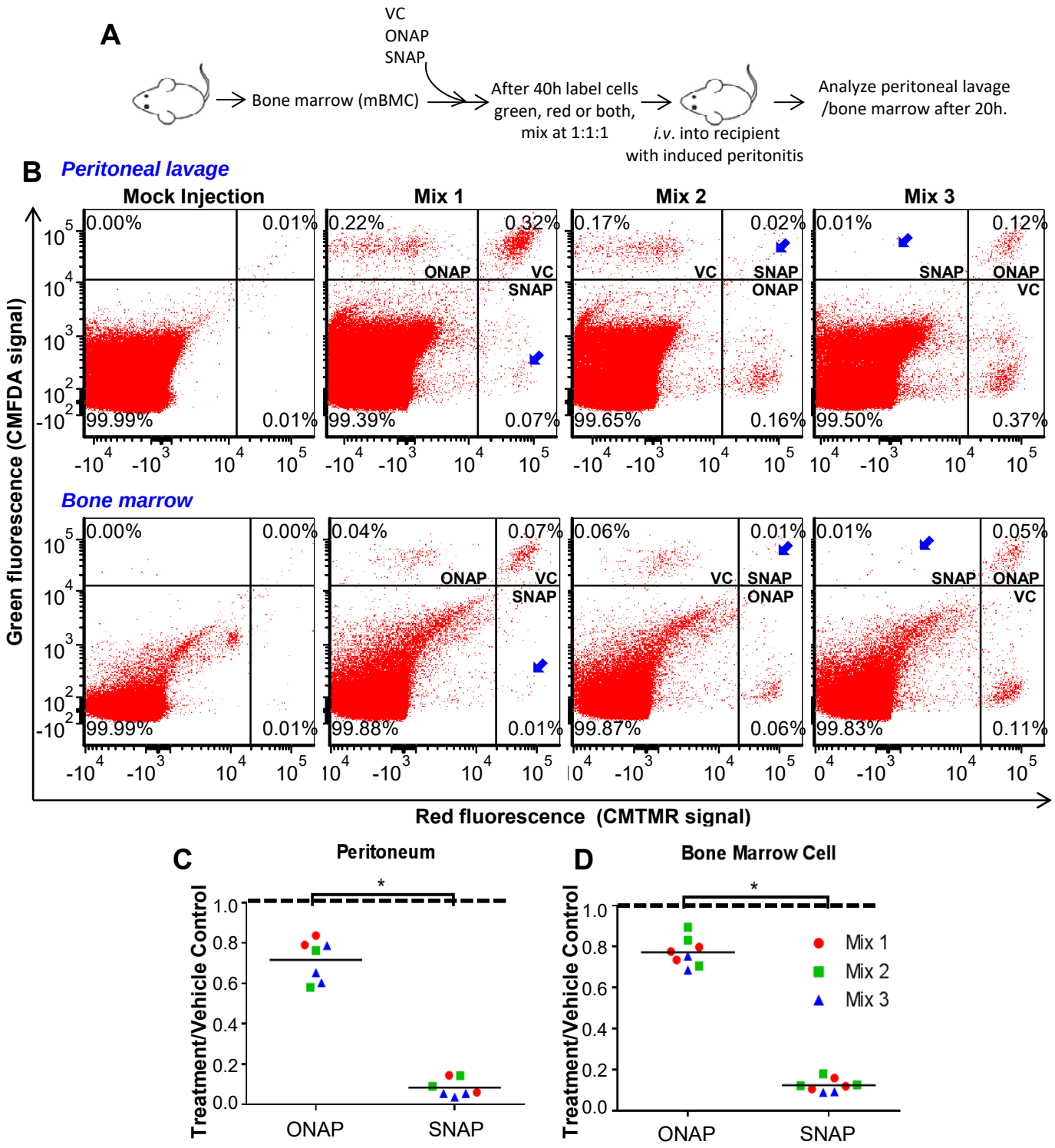
A
VC
ONAP
SNAP
Bone marrow (mBMC)
After 40h label cells green, red or both, mix at 1:1:1
i.v. into recipient with induced peritonitis
Analyze peritoneal lavage /bone marrow after 20h.
B
Peritoneal lavage
Mock Injection
Mix 1
Mix 2
Mix 3
Bone marrow
Green fluorescence (CMFDA signal)
Red fluorescence (CMTMR signal)
C
Peritoneum
Treatment/Vehicle Control
ONAP
SNAP
D
Bone Marrow Cell
Mix 1
Mix 2
Mix 3

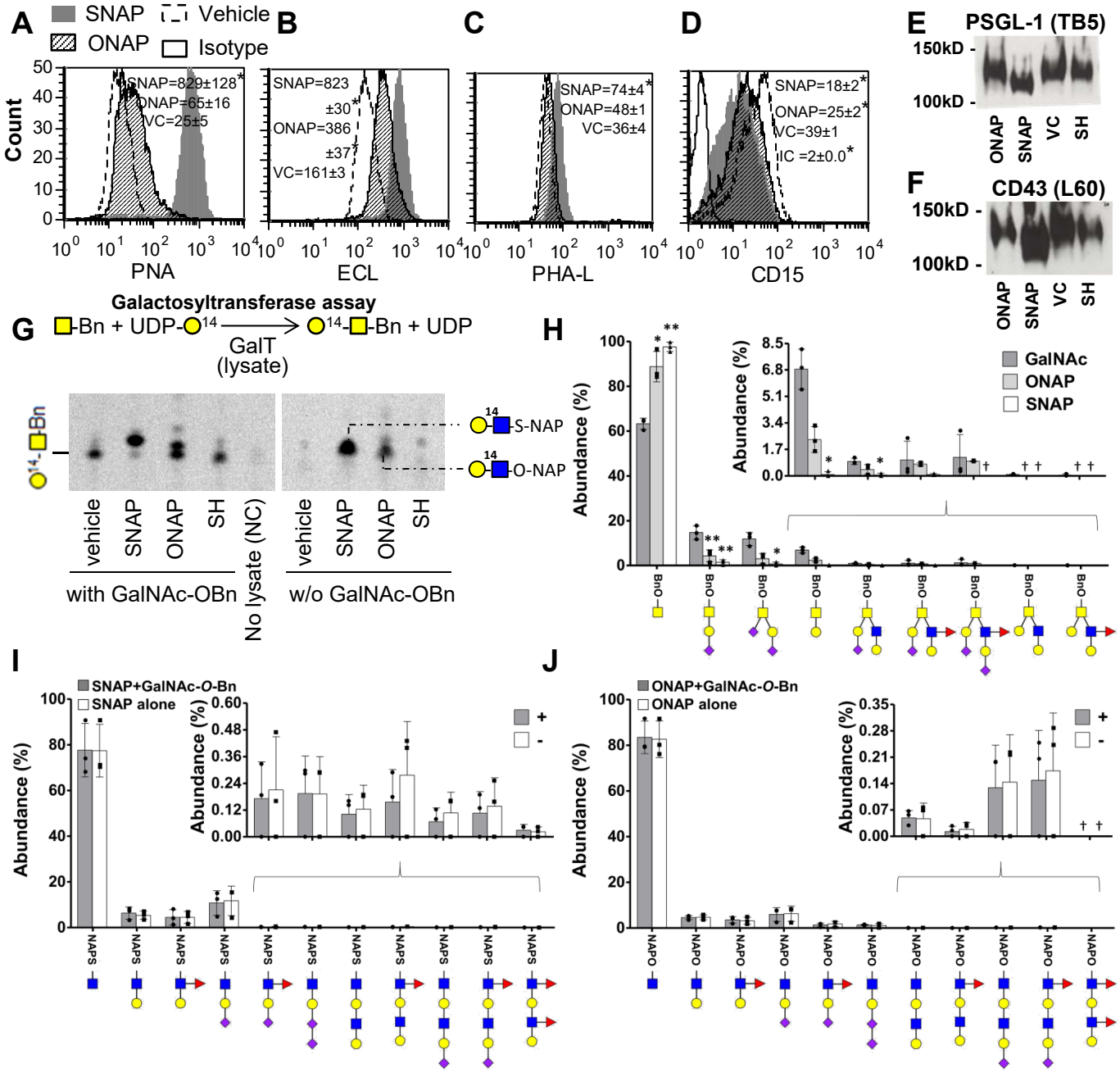
A
SNAP
ONAP
Vehicle
Isotype
Count
SNAP=829±128*
ONAP=65±16
VC=25±5
PNA
B
SNAP=823
±30*
ONAP=386
±37*
VC=161±3
ECL
C
SNAP=74±4*
ONAP=48±1
VC=36±4
PHA-L
D
SNAP=18±2*
ONAP=25±2*
VC=39±1
IC =2±0.0*
CD15
E
PSGL-1 (TB5)
150kD
100kD
ONAP
SNAP
VC
SH
F
CD43 (L60)
150kD
100kD
ONAP
SNAP
VC
SH
G
Galactosyltransferase assay
-Bn + UDP-
GalT
(lysate)
+ UDP
S-NAP
O-NAP
vehicle
SNAP
ONAP
SH
with GalNAc-OBn
No lysate (NC)
w/o GalNAc-OBn
H
Abundance (%)
GalNAc
ONAP
SNAP
I
SNAP+GalNAc-O-Bn
SNAP alone
Abundance (%)
J
ONAP+GalNAc-O-Bn
ONAP alone
Abundance (%)

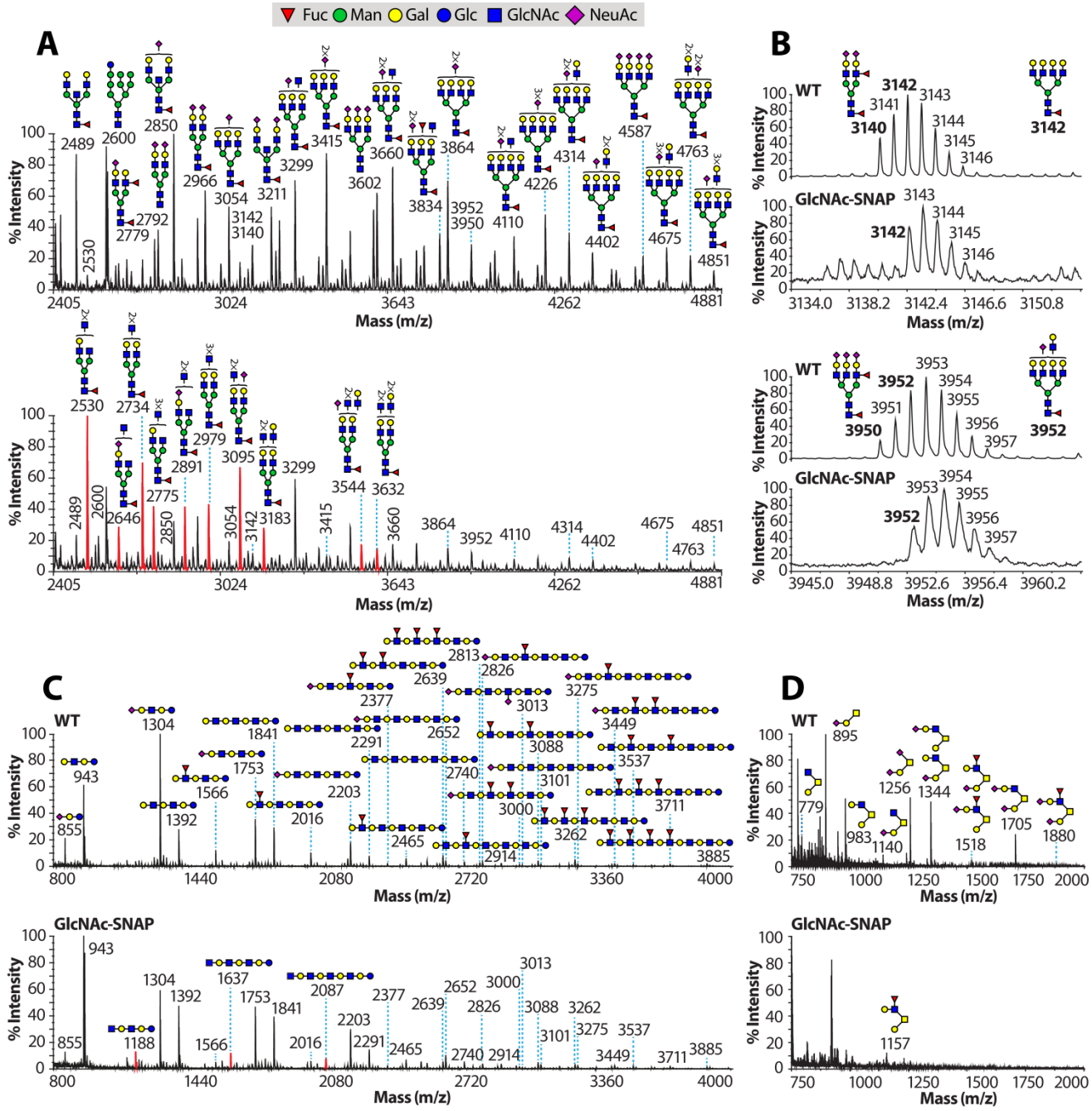
Fuc Man Gal Glc GlcNAc NeuAc
A
B
C
D
WT
GlcNAc-SNAP
% Intensity
Mass (m/z)

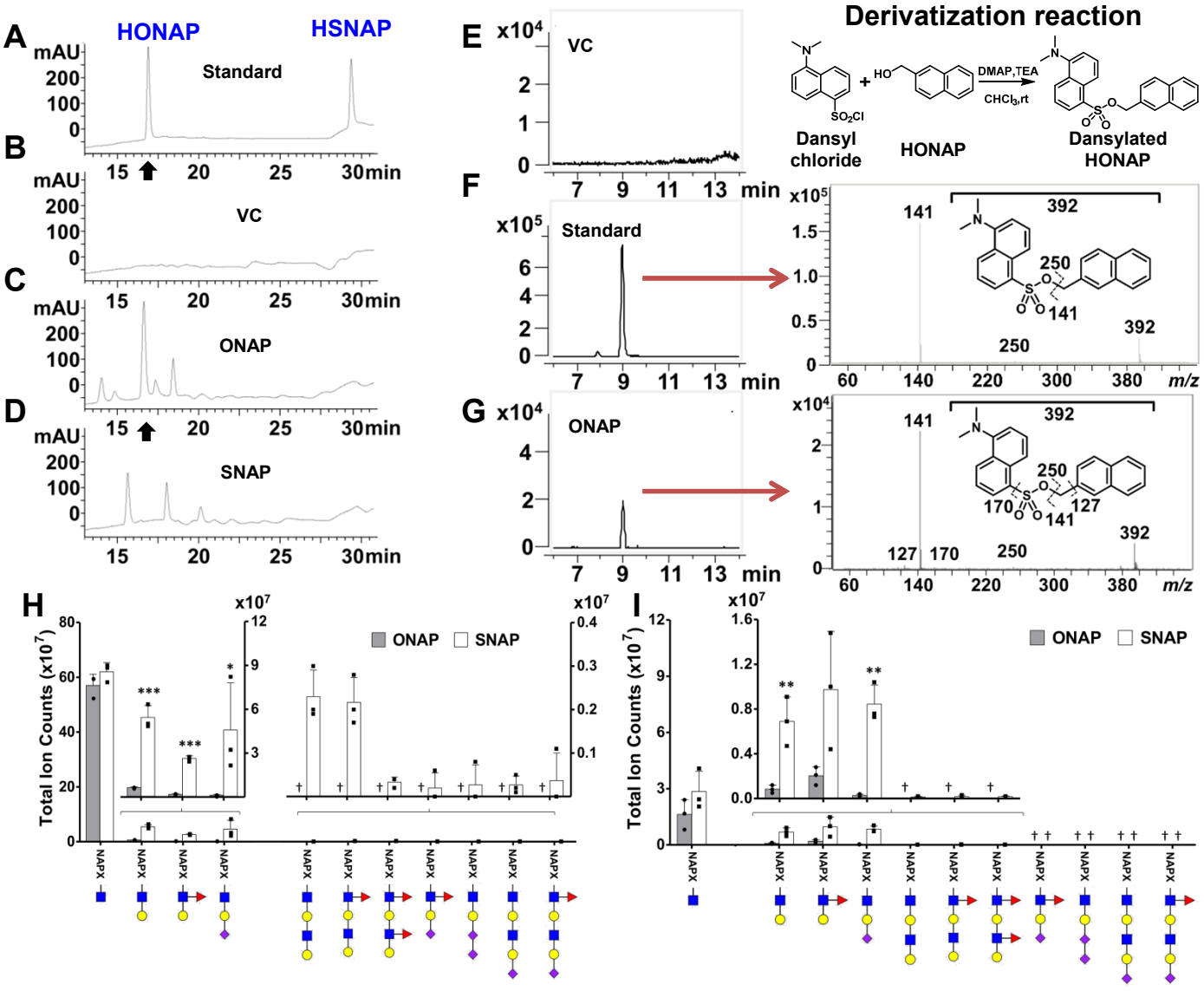
A
HONAP
HSNAP
mAU
Standard
B
VC
C
ONAP
D
SNAP
15
20
25
30min
E
x10^4
VC
F
x10^5
Standard
G
ONAP
7
9
11
13
min
Derivatization reaction
DMAP,TEA
CHCl3,rt
Dansyl chloride
HONAP
Dansylated HONAP
141
392
250
127
170
60
140
220
300
380
m/z
H
I
Total Ion Counts (x10^7)
ONAP
SNAP
NAPX

KEY RESOURCES TABLE

REAGENT or RESOURCE	SOURCE	IDENTIFIER
Antibodies		
HECA-452 (anti-human CLA)	BD Biosciences	RRID: AB_396243
D12 (anti-human CD11b)	BD Biosciences	RRID: AB_400112
HI98 (anti-human CD15)	BD Biosciences	RRID: AB_395801
KPL-1 (anti-human CD162)	BD Biosciences	RRID: AB_396324
DREG-56 (anti-human CD62L)	BD Biosciences	Cat#: 555544
L60 (anti-human CD43)	BD Biosciences	RRID: AB_394204
TB5 (anti-human CD162)	GeneTex	RRID: AB_377146
IA8 (anti-mouse Ly-6G)	BioLegend	RRID: AB_1877163
P2H3 (anti-human E-selectin)	Thermo Fisher Scientific	RRID: AB_11219468
G1 (anti-human CD62P)	Ancell	Cat#: 252-820
ECL lectin (Galβ1,4GlcNAc)	Vector Laboratories	RRID: AB_2336437
PHA-L lectin (binds complex glycan epitope: Galβ1,4GlcNAc β1,6(GlcNAc β1,2Manα1,3)Man α1,3)	Vector Laboratories	RRID: AB_2336655
MAL II lectin (binds α2,3sialic acid)	Vector Laboratories	RRID: AB_2336569
PNA lectin (binds Galβ1,3GalNAc)	Vector Laboratories	RRID: AB_2336458
VVA lectin (binds GalNAcα)	Vector Laboratories	RRID: AB_2336854
Chemicals, Peptides, and Recombinant Proteins		
LC/MS solvents and common chemicals	Sigma-Aldrich	
L-selectin	R&D Systems	728-LS-100
E-selectin	R&D Systems	724-ES-100
P-selectin	R&D Systems	137-PS-050
IL-1b	R&D Systems	201-LB-025/CF
PSGL-1 peptide (Custom synthesis)	GenScript	
Glycosides	Syntheses described in current manuscript	
Experimental Models: Cell Lines		
HL-60	ATCC	RRID: CVCL_0002
HL-60 Knock-outs	Stolfa, G. *et al Sci. Rep*. **2016**, 6:30392	
PC-3	ATCC	RRID: CVCL_0035
T-47D	ATCC	RRID: CVCL_0553
ZR-75-1	ATCC	RRID: CVCL_0588
HUVEC	ATCC	RRID: CVCL_2959
Experimental Models: Organisms/Strains		
mice	Envigo RMS	Catalog 44 C57BL/6 wild-type
Software and Algorithms		
DrawGlycan-NSFG	Cheng, K. *et al. Glycobiology* **2017**, 27(3): 200-205	https://github.com/kaichengub/DrawGlycan-SNFG https://VirtualGlycome.org/drawglycan
GlycoWorkbench	Ceroni, A. *et al. J. Proteome Res.* **2008**, 7(4):1650-9	https://github.com/alternativeTime/glycoworkbench

SUPPLEMENTAL DATA

Compound Characterization (Related to Figure 1 and Methods Details, Chemical synthesis)

Structural analysis of chemical compounds confirmed by NMR and MS analysis prior to their use in biochemical studies.

Supplemental Figure S1. (Related to Figure 2). Effect of ONAP and SNAP on CLA expression and selectin binding.

Supplemental Figure S2. (Related to Figure 2, 3). SNAP reduced E- and L-selectin IgG binding to differentiated HL-60s.

Supplemental Figure S3. (Related to Figure 5). Cell surface glycan modification after treatment with different analogs.

Supplemental Figure S4. (Related to Figure 5). SNAP effect on lectin binding to various cell types.

Supplemental Figure S5. (Related to Figure 5) SNAP effect on O-glycosylation and ppGalNAcT activity.

Supplemental Figure S6. (Related to Figure 5). Effect of glycosides on VVA-lectin binding.

Supplemental Figure S7. (Related to Figure 7). SNAP and ONAP serves as surrogate acceptors in cells (Independent validation studies).

Compound Characterization

1-(Naphthalen-2-ylmethanol) 2-Acetamido-3,4,6-tri-*O*-Acetyl-2-Deoxy-1-Thio-β-D-Glucopyranoside (1). The product was obtained following the procedure previously reported as white solid. *^{1}H NMR* (400 MHz, $CDCl_3$) δ 7.85-7.78 (m, 3H), 7.70 (s, 1H), 7.52-7.44 (m, 3H), 5.18 (d, *J* = 7.9 Hz, 1H), 5.09 (d, *J* = 9.7 Hz, 1H), 4.93 (t, *J* = 9.2 Hz, 1H), 4.28-4.15 (m, 4H), 4.12 (AB syst., *J* = 13.1 Hz, 1H), 3.96 (AB syst., *J* = 13.0 Hz, 1H), 3.54 (ddd, *J* = 7.6, 5.2, 2.6 Hz, 1H), 2.14 (s, 3H), 2.00 (s, 3H), 1.99 (s, 3H), 1.90 (s, 3H). *MS^1 and MS^2*. Fragments were generated in positive ionization mode. $[M+H]^+$ *m/z*: observed 504.16840; theoretical 504.16866. Observed fragments: 462.21225, 443.97440, 384.14798, 366.20688, 330.10626, 324.10376, 290.24631, 282.12305, 270.02261, 248.20908, 210.07373, 168.05301, 149.85677, 141.06970.

1-(Naphthalen-2-ylmethanol) 2-Acetamido-2-Deoxy-1-Thio-β-D-Glucopyranoside (2). The product was obtained following the procedure previously reported above as white solid. *^{1}H NMR* (400 MHz, CD_3OD) δ 7.84-7.81 (m, 4H), 7.52-7.44 (m, 3H), 4.23 (AB syst., *J* = 13.0 Hz, 1H), 4.22 (d, *J* = 10.3 Hz, 1H), 3.97 (AB syst., *J* = 12.9 Hz, 1H), 3.96 (dd, *J* = 12.1, 2.0 Hz, 1H), 3.86 (t, *J* = 9.9 Hz, 1H), 3.73 (dd, *J* = 12.1, 6.3 Hz, 1H), 3.30-3.26 (m, 2H), 3.54 (ddd, *J* = 7.6, 5.2, 2.6 Hz, 1H), 1.92 (s, 3H). *MS^1 and MS^2*. Fragments were generated in positive ionization mode. $[M+H]^+$ *m/z*: observed 378.13660; theoretical 378.13697. Observed fragments: 300.27072, 204.02351, 185.97626, 168.02682, 143.96878, 125.91946.

Geranyl 2-Acetamido-3,4,6-tri-*O*-Acetyl-2-Deoxy-1-Thio-β-D-Glucopyranoside (3). The product was obtained following the procedure previously reported above as white solid. *^{1}H NMR* (400 MHz, $CDCl_3$) δ 5.52 (t, *J* = 9.1 Hz, 1H), 5.18 (t, *J* = 8.1 Hz, 1H), 5.12-5.04 (m, 3H), 4.46 (d, *J* = 10.2 Hz, 1H), 4.21 (dd, *J* = 12.2, 5.3 Hz, 1H), 4.15-4.07 (m, 2H), 3.91-3.73 (m, 3H), 3.58 (ddd, *J* = 7.3, 5.0, 2.4 Hz, 1H), 3.50-3.42 (m, 1H), 3.14 (dd, *J* = 13.1, 6.6, 1H), 2.06 (s, 3H), 2.01 (s, 6H), 1.94 (s, 3H), 1.68 (s, 3H), 1.64 (s, 3H), 1.60 (s, 3H). *MS^1 and MS^2*. Fragments were generated in positive ionization mode. $[M+H]^+$ *m/z*: observed 500.23111; theoretical 500.23126. Observed fragments: 482.27631, 440.14297, 414.29739, 380.27087, 364.1364, 362.28607, 330.11551, 320.19153, 302.13629, 270.06577, 260.27185, 210.03888, 168.08176,149.86636

Geranyl 2-Acetamido-2-Deoxy-1-Thio-β-D-Glucopyranoside (4). The product was obtained following the procedure previously reported above as yellowish solid. *^{1}H NMR* (400 MHz, CD_3OD) δ 5.50 (t, *J* = 7.5 Hz, 1H), 5.08 (tt, *J* = 8.5, 1.5 Hz, 1H), 4.39 (d, *J* = 10.3 Hz, 1H), 3.85 (dd, *J* = 12.0, 2.4 Hz, 1H), 3.75 (t, *J* = 9.9 Hz, 1H), 3.67 (dd, *J* = 12.2, 5.7 Hz, 1H), 3.49 (dd, *J* = 12.8, 9.0 Hz, 1H), 3.43-3.33 (m, 2H), 3.21-3.19 (m, 2H), 2.14-1.99 (m, 2H), 1.95 (s, 6H), 1.75-1.70 (m, 1H), 1.66 (s, 3H), 1.60 (s, 3H), 1.29-1.26 (m, 1H). *MS^1 and MS^2*. Fragments were generated in positive ionization mode. $[M+H]^+$ *m/z*: observed 374.20041; theoretical 374.19957. Observed fragments: 356.33224, 238.10071, 204.13142, 186.04022, 168.01074, 143.99771, 125.92296.

8-Bromooctyl 2-Acetamido-3,4,6-tri-*O*-Acetyl-2-Deoxy-1-Thio-β-D-Glucopyranoside (5). The product was obtained following the procedure previously reported above as white solid. *^{1}H NMR* (400 MHz, $CDCl_3$) δ 5.41 (d, *J* = 9.3 Hz, 1H), 5.16 (t, *J* = 9.7 Hz, 1H), 5.09 (t, *J* = 9.5 Hz, 1H), 4.56 (d, *J* = 10.2 Hz, 1H), 4.23 (dd, *J* = 12.3, 4.9 Hz, 1H), 4.18-4.06 (m, 2H), 3.68 (ddd, *J* = 10.0, 5.1, 2.4 Hz, 1H), 3.40 (t, *J* = 6.2 Hz, 2H), 2.74-2.62 (m, 2H), 2.08 (s, 3H), 2.03 (s, 3H), 2.02 (s, 3H), 1.96 (s, 3H), 1.84 (quint, *J* = 7.2 Hz, 2H), 1.63-1.57 (m, 2H), 1.43-1.30 (m, 8H). *MS^1 and MS^2*. Fragments were generated in positive ionization mode. $[M+H]^+$ *m/z*: observed 554.14246; theoretical 554.14178. Observed fragments: 536.19055, 494.06061, 416.34119, 374.18787, 330.07739, 269.96057, 210.02907, 167.95576.

1-(Naphthalen-2-ylmethanol) 2-Acetamido-3,4,6-tri-*O*-Acetyl-2-Deoxy-β-D-Glucopyranoside (6). The product was obtained following the procedure previously reported above as white solid. *^{1}H NMR* (400 MHz, $CDCl_3$) δ 7.84-7.80 (m, 3H), 7.75 (s, 1H), 7.51-7.41 (m, 3H), 5.27 (d, *J* = 8.8 Hz, 1H), 5.20-5.04 (m, 3H), 4.77 (d, *J* = 12.7 Hz, 1H), 4.66 (d, *J* = 8.3 Hz, 1H), 4.30 (dd, *J* = 12.1, 4.6 Hz, 1H), 4.19 (d, *J* = 12.1 Hz, 1H), 4.00 (q, *J* = 8.6 Hz, 1H), 3.70-3.65 (m, 1H), 2.11 (s, 3H), 2.01 (s, 6H), 1.91 (s, 3H). *MS^1 and MS^2*. Fragments were generated in positive ionization mode. $[M+H]^+$ *m/z*: observed 488.19110; theoretical 488.19151. Observed fragments: 470.25247, 446.37146, 428.18890, 368.27975, 330.05261, 269.82465, 210.11472, 168.11179, 149.96254, 140.98838.

1-(Naphthalen-2-ylmethanol) 2-Acetamido-2-Deoxy-β-D-Glucopyranoside (7). The product was obtained following the procedure previously reported above as white solid. *^{1}H NMR* (400 MHz, CD_3OD) δ 7.86-7.82 (m, 4H), 7.49-7.46 (m, 3H), 5.06 (d, *J* = 12.4 Hz, 1H), 4.80 (d, *J* = 12.4 Hz, 1H), 4.53 (d, *J* = 8.4

Hz, 1H), 3.95 (d, *J* = 11.8 Hz, 1H), 3.80-3.72 (m, 2H), 3.42 (t, *J* = 9.4 Hz, 1H), 3.38-3.33 (m, 2H), 1.98 (s, 3H). *MS¹ and MS²*. Fragments were generated in positive ionization mode. $[M+H]^+$ *m/z*: observed 362.16089; theoretical 362.15981. Observed fragments: 344.10538, 326.16821, 267.12933, 249.14832, 204.01276, 186.04469, 167.94849, 144.11374, 141.11943, 126.01475.

***p*-Methoxyphenyl 2-Acetamido-3,4,6-tri-*O*-Acetyl-2-Deoxy-β-D-Glucopyranoside (8).** The product was obtained following the procedure previously reported above as white solid. *¹H NMR* (400 MHz, $CDCl_3$) δ 6.92 (d, *J* = 8.7 Hz, 2H), 6.78 (d, *J* = 8.7 Hz, 2H), 5.55 (d, *J* = 8.8 Hz, 1H), 5.37 (t, *J* = 9.9 Hz, 1H), 5.14-5.09 (m, 2H), (dd, *J* = 12.3, 5.4 Hz, 1H), 4.15-4.03 (m, 2H), 3.75 (s, 3H), 2.06 (s, 3H), 2.04 (s, 3H), 2.02 (s, 3H), 1.96 (s, 3H). *MS¹ and MS²*. Fragments were generated in positive ionization mode. $[M+H]^+$ *m/z*: observed 454.17038; theoretical 454.17077. Observed fragments: 436.14349, 330.17300, 270.17480, 210.07660, 168.04672, 149.95697.

***p*-Methoxyphenyl 2-Acetamido-2-Deoxy-β-D-Glucopyranoside (9).** The product was obtained following the procedure previously reported above as white solid. *¹H NMR* (400 MHz, CD_3OD) δ 6.94 (d, *J* = 9.1 Hz, 2H), 6.79 (d, *J* = 9.1 Hz, 2H), 5.66 (d, *J* = 8.8 Hz, 1H), 5.38 (t, *J* = 9.8 Hz, 1H), 5.16-5.10 (m, 2H), 4.28 (dd, *J* = 12.2, 5.4 Hz, 1H), 4.18-4.05 (m, 2), 3.83-3.79 (m, 1H), 3.76 (s, 3H), 2.08 (s, 3H), 2.06 (s, 3H), 2.04 (s, 3H), 1.97 (s, 3H). *MS¹ and MS²*. Fragments were generated in positive ionization mode. $[M+H]^+$ *m/z*: observed 328.13916; theoretical 328.13908. Observed fragments: 310.24176, 251.00214, 203.89297, 185.88744, 167.88394, 144.12300.

Geranyl 2-Acetamido-2-Deoxy-β-D-Glucopyranoside (10). The product was obtained following the procedure previously reported above as yellowish solid. *¹H NMR* (400 MHz, CD_3OD) δ 5.28 (t, *J* = 6.3 Hz, 1H), 5.09 (t, *J* = 3.4 Hz, 1H), 4.42 (d, *J* = 8.4 Hz, 1H), 4.28 (dd, *J* = 11.7, 6.2 Hz, 1H), 4.15 (dd, *J* = 11.8, 7.5 Hz, 1H), 3.88-3.71 (m, 2H), 3.71-3.55 (m, 2H), 3.45-3.41 (m, 2H), 3.35-3.21 (m, 2H), 3.21-3.19 (m, 2H), 2.10-1.99 (m, 2H), 1.98 (s, 3H), 1.96 (s, 3H), 1.66 (s, 3H), 1.59 (s, 3H), 1.27-1.10 (m, 2H). *MS¹ and MS²*. Fragments were generated in positive ionization mode. $[M+H]^+$ *m/z*: observed 358.22229; theoretical 358.22241. Observed fragments: 340.15756, 221.92007, 203.97479, 186.00990, 167.95898, 143.96048, 125.93074.

Benzyl 2-Acetamido-2-Deoxy-β-D-Glucopyranoside (11). The product was obtained following the procedure previously reported above as white solid. *^{1}H NMR* (400 MHz, CD_3OD) δ 7.35-7.27 (m, 5H), 4.91 (d, *J* = 12.1 Hz, 1H), 4.64 (d, *J* = 12.1 Hz, 1H), 4.50 (d, *J* = 8.4 Hz, 1H), 3.94 (dd, *J* = 11.9, 2.0 Hz, 1H), 3.78-3.72 (m, 2H), 3.48 (dd, *J* = 10.3, 8.4 Hz, 1H), 3.39-3.29 (m, 2H), 1.98 (s, 3H). *MS^1 and MS^2*. Fragments were generated in positive ionization mode. $[M+H]^+$ *m/z*: observed 312.14417; theoretical 312.14416. Observed fragments: 294.08081, 203.99313, 186.05736, 167.88780, 126.00682.

2-Acetamido-3,4,6-tri-*O*-Acetyl-2-Deoxy-1-Thio-β-D-Glucopyranoside (12). The product was obtained following the procedure previously reported above as white solid. *^{1}H NMR* (400 MHz, $CDCl_3$) δ 5.63 (d, *J* = 9.2 Hz, 1H), 5.19-5.01 (m, 2H), 4.57 (t, *J* = 9.7 Hz, 1H), 4.23 (ddd, *J* = 12.4, 4.9, 2.2 Hz, 1H), 4.18-4.06 (m, 2H), 3.68 (ddd, *J* = 7.2, 4.9, 2.3 Hz, 1H), 2.56 (dd, *J* = 9.4, 2.3 Hz, 1H), 2.09 (s, 3H), 2.04 (s, 3H), 2.02 (s, 3H), 1.98 (s, 3H). *MS^1 and MS^2*. Fragments were generated in positive ionization mode. $[M+H]^+$ *m/z*: observed 364.10577; theoretical 364.10606. Observed fragments: 346.13809, 330.08887, 322.08908, 304.00058, 269.98792, 244.16260, 226.10577, 209.99199, 184.07031, 168.06059, 149.9760, 141.98468, 124.79923.

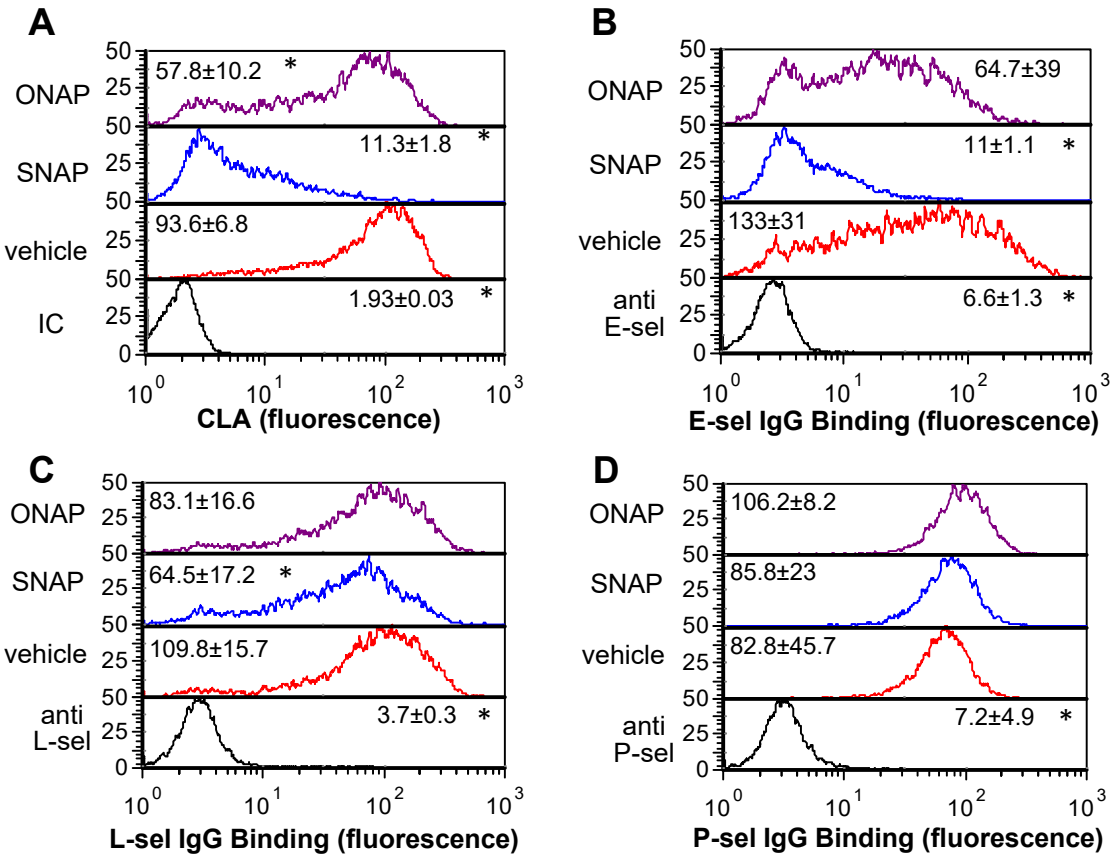

Supplemental Figure S1. (Related to Figure 2). Effect of ONAP and SNAP on CLA expression and selectin binding. Cytometry histogram of CLA/sLe^X epitope expression and selectin binding after treatment of HL-60s with 100μM SNAP, ONAP or vehicle control for 40h: **A.** CLA (mAb HECA-452) epitope expression, **B.** E-selectin-IgG **C.** L-selectin-IgG, and **D.** P-selectin-IgG binding. Binding specificity was confirmed using anti-selectin blocking mAbs against E-selectin (clone P2H3), L-selectin (Dreg-56), and P-selectin (G1), to block selectin-IgG binding to vehicle treated cells. Experimental method is identical to Fig. 2 (main manuscript). Error bars are standard deviation. * $P<0.05$ with respect to vehicle control. SNAP significantly reduced E- and L-selectin IgG binding and CLA expression on cell surface.

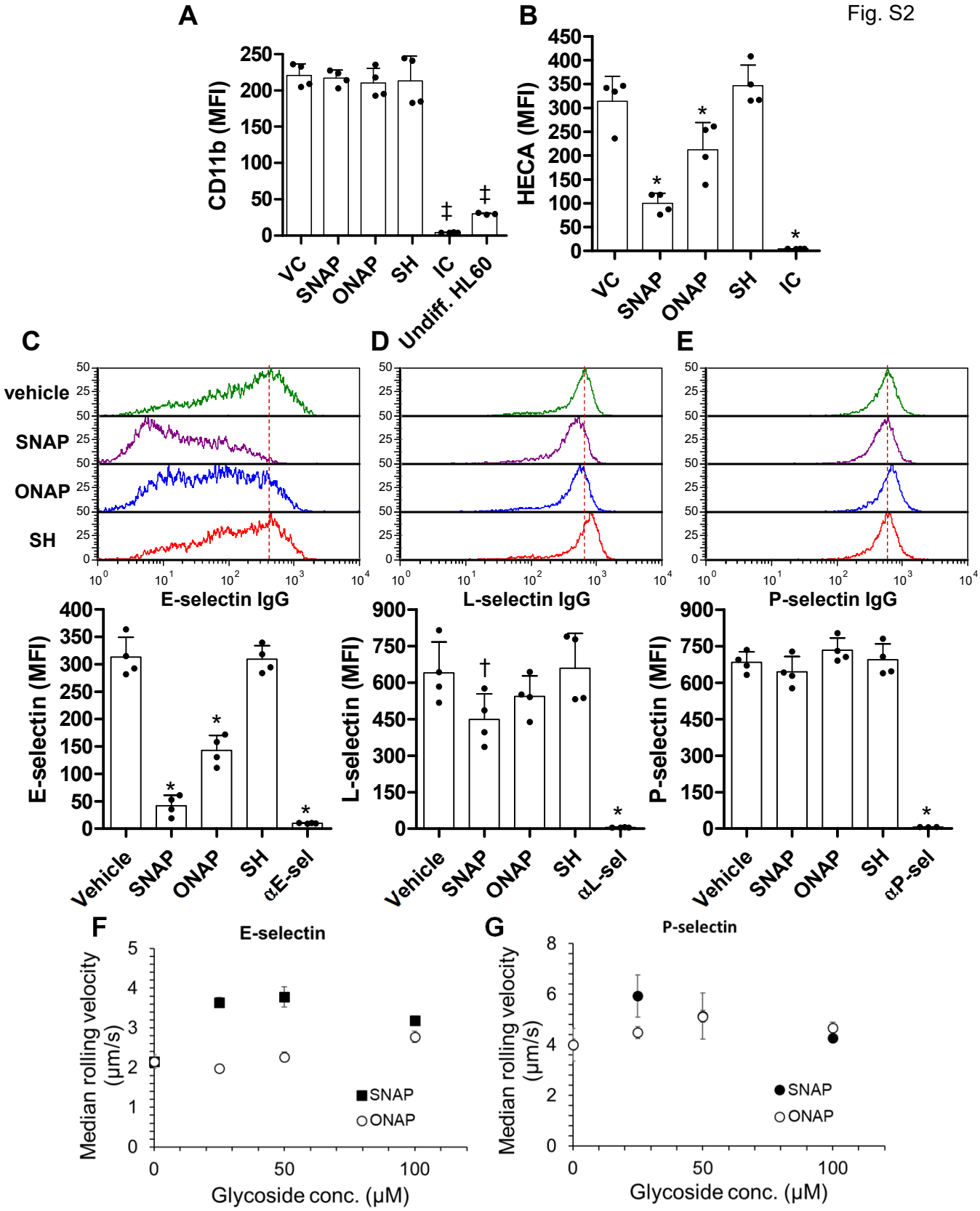

Supplemental Figure S2. (Related to Figure 2, 3). SNAP reduced E- and L-selectin binding. **A.-E.** 1.3% DMSO was added to HL-60 cell culture medium to trigger terminal differentiation to neutrophils over 5-days. 80μM SNAP, ONAP and SH were added on day 3. **A.** On day 5, CD11b was augmented by 5-fold independent of treatment, compared to undifferentiated HL60s. **B.** HECA-452 epitope expression was reduced upon SNAP treatment. **C-E.** E-selectin IgG binding to HL60s differentiated to neutrophils was also decreased upon SNAP treatment with a smaller effect of ONAP (panel **C**). L- selectin-IgG binding was partially diminished by SNAP (**D**), with no effect on P-selectin IgG binding (**E**). **F.-G.** Undifferentiated HL-60s cultured with different conc. of glycosides were rolled on selectin substrates at 1 dyn/cm^2. SNAP more prominently increased rolling velocity on E-selectin. ‡ P<0.05 with respect to all other treatments except that there is no difference between ‡. * P<0.05 with respect to all other treatments in that panel. † P<0.5 with respect to all other treatments except ONAP. MFI: Mean fluorescence intensity.

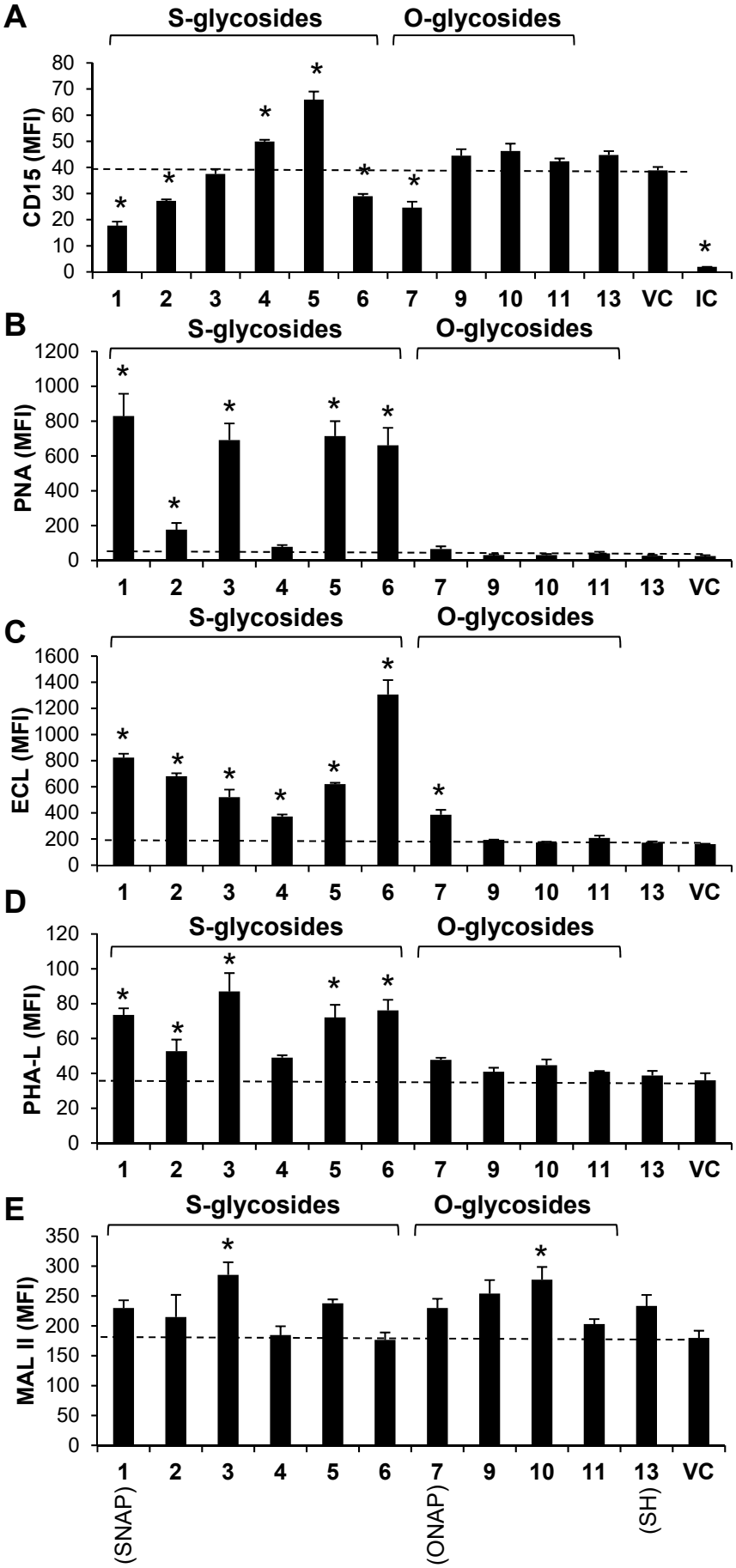

Supplemental Figure S3. (Related to Figure 5). Cell surface glycan modification after treatment with different analogs. HL60s were treated with glycosides/decoys or VC (0.25%DMSO) prior to cytometry analysis using a set of fluorescent mAbs and lectins: **A.** CD15/Lewis-X (mAb HI98), **B.** PNA (binds Galβ1,3GalNAc), **C.** ECL (binds Galβ1,4GlcNAc), **D.** PHA-L (binds branched N-glycans), and **E.** MAL-II (binds α2,3-linked sialic acid). IC: isotype control. S-glycosides increase PNA, ECL and PHA-L lectin binding, with smaller effect on the CD15 and MAL-II epitopes. * $P<0.05$ with respect to VC (levels indicated using dashed line).

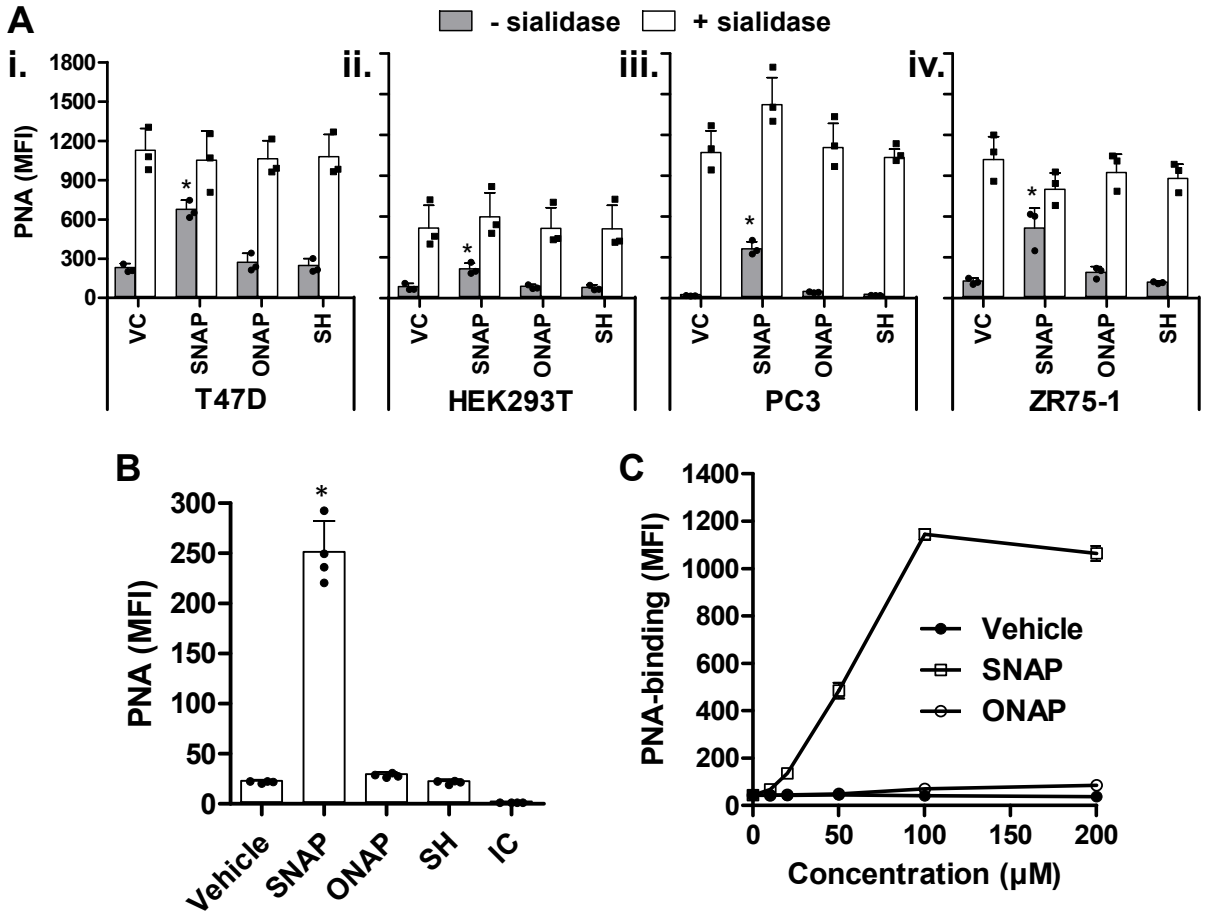

Supplemental Figure S4. (Related to Figure 5). SNAP effect on lectin binding to various cell types: A. T47D (breast, **i.**), HEK293T (kidney, **ii.**), PC3 (prostate, **iii.**) or ZR75-1 (breast, **iv.**) cells were cultured with 80μM ONAP, SNAP, SH, or VC (0.2%DMSO) for 40h. PNA-lectin binding was upregulated by SNAP (but not ONAP) in all cancer cell lines tested (* $P<0.05$). Measurements were performed prior to and after sialidase treatment to remove cell-surface sialic acids. **B.** 80μM ONAP, SNAP and controls were added to HL-60s that were being terminally differentiated to neutrophils over 5-days by addition of 1.3% DMSO to cell culture medium. PNA-lectin binding to differentiated cells was prominently upregulated by SNAP, but not ONAP or other control treatments (* $P<0.05$). Error bars are very small in some cases. **C.** HL60s were cultured with SNAP or ONAP at various concentrations (0-200μM). At t=40h, FITC conjugated PNA binding was measured using flow cytometry. This dosage study suggests that SNAP is active at concentrations as low as 20μM and reaches maximum function at ~100μM.

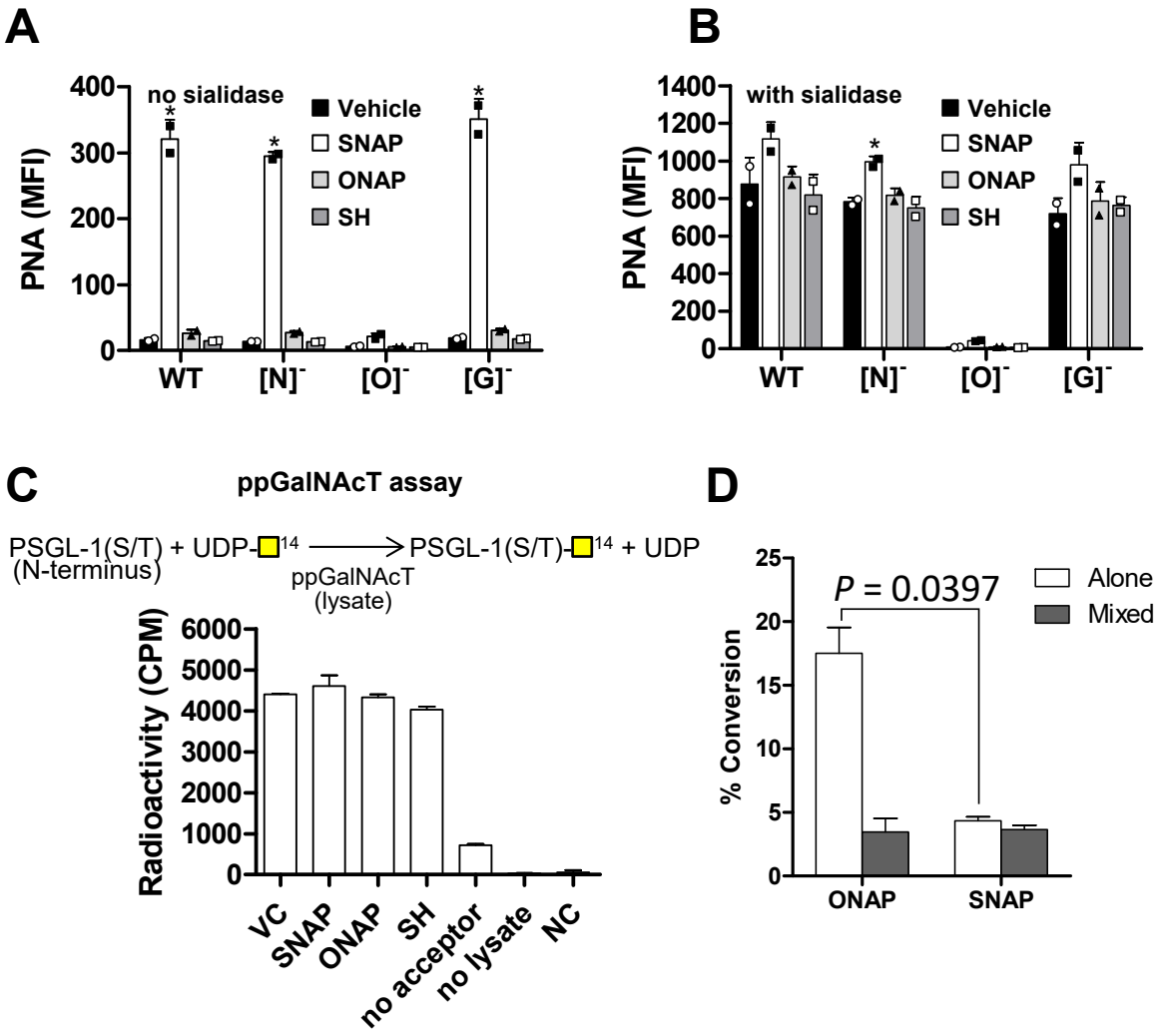

Supplemental Figure S5. (Related to Figure 5) SNAP effect on O-glycosylation and ppGalNAcT activity A-B. PNA binding to HL-60s and CRISPR-Cas9 mutants lacking extended O-glycans ([O]-), N-glycans ([N]-) or glycosphingolipids ([G]-), after 40h culture with 80μM ONAP, SNAP, SH or vehicle. These CRISPR-Cas9 isogenic clones are described elsewhere (Stolfa *et al.*, 2016). Lectin-binding was performed prior to (panel **A**) or after (**B**) treatment with 5U/mL α2,3/6/8/9-neuraminidase from *Arthrobacter ureafaciens* for 1h at 37°C. Here, SNAP increased PNA binding to all HL-60s except the $[O]^{-}$ cells that lack functional core-1 GalT activity. Additionally, sialidase treatment increased PNA-binding to all cells, except the $[O]^{-}$ cells. The data confirm that changes in PNA-lectin binding report on alterations in O-glycan biosynthesis only. **P*<0.05 with respect to all other treatments (error bars are S.D.). **C.** Enzymology assays measured ppGalNActransferase activity. Here, HL-60 lysates from cells treated with 80μM SNAP, ONAP, SH, or VC (0.2% DMSO) were mixed with synthetic acceptor/PSGL-1 peptide and radioactive nucleotide-sugar donor/[C^{14}]UDP-GalNAc. Control runs had either no-acceptor or no cell lysate. ppGalNAcT activity was unaltered by O- and S-glycoside decoys. **D.** GalT activity were measured using ONAP/SNAP substrate, 1 mM UDP-Gal, and 60 μg of protein from cell lysate. Studies were performed using 500 μM ONAP alone, 500 μM SNAP alone or 500 μM ONAP + 500 μM SNAP mixture (grey bar). Reaction products were resolved using LC-MS and verified using MS/MS. % Conversion was calculated based on area under the intensity vs. time curve. SNAP is a poorer decoy substrate compared to ONAP. SNAP reduced Gal addition to ONAP, in competition/mixture assays.

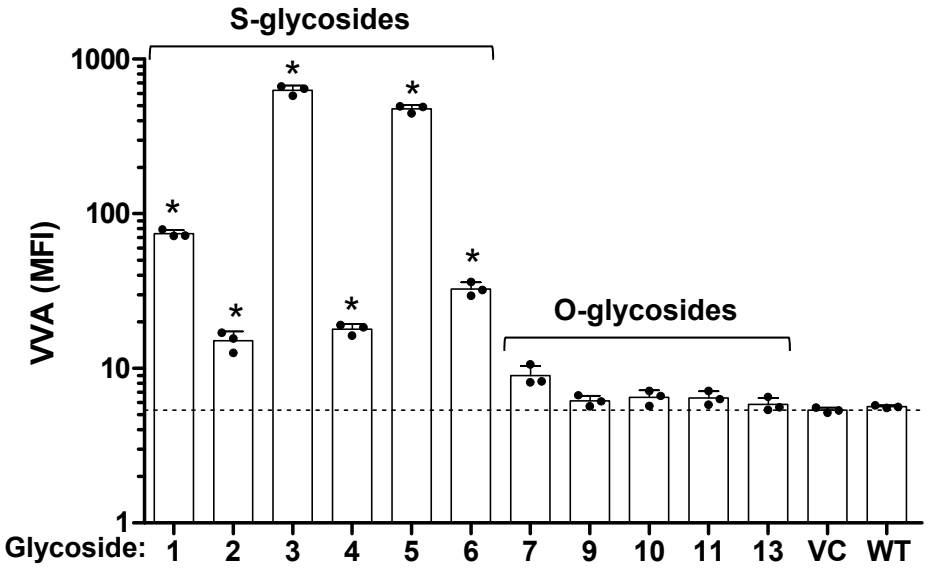

Supplemental Figure S6. (Related to Figure 5). Effect of glycosides on VVA-lectin binding. Wild-type HL-60s were cultured with 80μM ONAP (**7**), SNAP (**1**) or vehicle controls for 40h. Flow cytometry analysis was performed identical to Fig. 5 (main manuscript) to assay changes in VVA-lectin binding following glycoside treatment. * $P<0.05$ with respect to VC. SNAP (**1**) increased VVA-lectin binding indicating glycan truncation at the Tn-antigen (GalNAcα) stage.

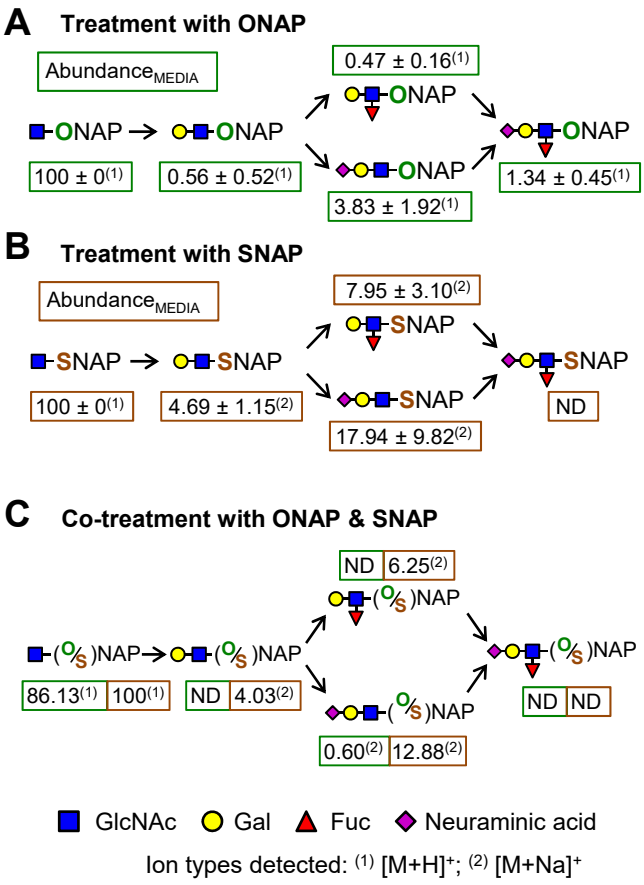

Supplemental Figure S7. (Related to Figure 7). SNAP and ONAP serves as surrogate acceptors in cells (Independent validation studies). ESI-qTOF LC-MS/MS was performed to analyze culture media from HL60s treated with either 60μM ONAP (**A**), SNAP (**B**) or both at 1:1 ratio (**C**). Ion counts are reported relative to the most abundant glycan: Thus,100 = 5.3×10^6 counts for panel A, 1.2×10^6 counts for B and 4.6×10^6 counts for C. All structures were validated using MS/MS. ND = not detected. SNAP and ONAP both served as surrogate acceptors, with SNAP being the more efficient one. Findings are consistent with independent studies described in main manuscript, performed using Orbitrap detector.